

Charge Separation in Heteroleptic Cu (I) Donor-Chromophore-Acceptor Triads Involving 2,9-disubstituted 1,10-phenanthroline Ligands

Megan Lazorski

Colorado State University

Fort Collins, CO 80523

Introduction and Background

Photosynthesis is arguably one of the most important biological processes in nature.^{1,2} Not only does photosynthesis convert light energy into chemical energy, this conversion occurs through a sophisticated sequence of events that execute non-trivial thermodynamic processes such as carbon fixation (reduction of CO₂) and water oxidation.¹⁻³ Several of the events in the photosynthetic process have been researched heavily for their obvious application to solar energy harvesting capabilities.²⁻⁶ Not only could the development of an artificial photosynthesis system lead to new types of solar cells, but also solar powered water splitting, and a host of other electron transfer devices.^{2,4,6} One of the fundamental processes of photosynthesis that researchers have studied in order to create an artificial photosynthetic system is the photoinduced charge separated state.^{3,4,7,8}

Charge-separated states (CSS) can be achieved in systems that incorporate a chromophoric component with a donor moiety (D) and/or an acceptor moiety (A).

There are two general types of CSS systems. The first type utilizes molecules with extended conjugated π systems as the chromophore, such as porphyrins, carotenoids, and fullerenes.^{3,8,9} The second type of CSS system utilizes a metal chromophore that exhibits a strong absorption in the visible.^{3,8,9} When the system contains both a D and an A moiety it is called a Donor-Chromophore-Acceptor (D-C-A) triad. The focus of this research is the metal containing D-C-A triads where the chromophore is Ru or Cu and the D and A moieties are based on a bipyridine (bpy) or phenanthroline (phen) with phenothiazine-type (PXZ, donor) and diquat (DQ²⁺, acceptor) functionalization, which will be referred to as D-C²⁺-A²⁺ for brevity.^{7,9-16}

D-C-A triads can achieve a CSS by an electron transport mechanism similar to photosynthetic systems. A photon of light excites the chromophoric metal center to a triplet metal-to-ligand charge-transfer state (³MLCT).⁹ The excited chromophore is now highly reducing and reduces the acceptor via a one-electron transfer process, which is called oxidative quenching.⁹ The oxidized

chromophore can now oxidize the donor, creating a di-radical CSS.⁹

Although this process may seem straight forward, many factors influence the formation of a long-lived CSS with a good quantum yield. CSS complexes are often very unpredictable.^{3,8,9} The inability to predict the formation of the CSS state is an artifact of its di-radical nature. The CSS state is sought after for its chemical potential and inherent reactivity, but these attributes can also destroy the CSS complex itself. Several electron transfer processes are in competition in the CSS and the relative rate constants of these electron transfer processes dictate whether the lifetime and quantum yield of the CSS will be enhanced or inhibited.^{3,8,9} The most influential electron transfer processes are: photoinitiated electron transfer to the $D-C^{2+}-A^{+}$ state, photophysical decay to the ground state, CSS recombination causing thermal relaxation to the ground state, and a second electron transfer to form $D^{+}\cdot-C^{+}-A^{+}$.^{3,7-9} A schematic diagram of the electron transfer processes in the D-C-A complexes is shown in Figure 1.

Understanding the factors that influence the electron transfer processes is key to designing a successful CSS in a D-C-A complex. Fortunately, many studies have

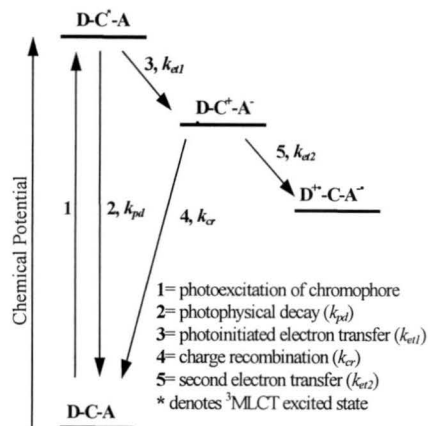


Figure 1. A simple representation of the competing electron transfer processes in D-C-A triads. Adapted from ref 8 and 9.

been performed to elucidate the issues that influence electron transport in CSS complexes. Research suggests that the free energy of the reaction and the reorganizational energy have the largest influence on the rates of electron transfer in the D-C-A triads.^{3,7-9,17-19} Furthermore, the relationship between free energy of the reaction and rates of electron transfer have been shown to satisfy equation 1 through theoretical modeling studies.^{3,8,17,19}

$$k_{et} = \frac{2\pi}{\hbar} V_{DA}^2 \left(\frac{1}{(4\pi\lambda k_b T)^{1/2}} \right) e^{-(\Delta G^0 + \lambda)^2 / 4\lambda k_b T} \quad (1)$$

In eq 1 k_{et} represents the rate of electron transfer, V_{DA} represents the amount of electronic coupling between the radical donor and acceptor electrons, λ represents the degree of reorganizational energy of both the solvent and the D-C-A triad, and finally ΔG^0 represents the free energy of

electron transfer reaction.^{3,8,17,19} Since the ΔG° term is in an exponential term, eq 1 relates that the k_{et} exhibits nonlinear dependence on the free energy.^{3,8,9,17-19}

In addition to ΔG° , it can be seen from eq 1 that the rate of electron transfer depends on several factors. The electronic coupling between the radical electrons on the D and A (V_{DA}) is an important contributor to the k_{et} .^{3,17} The V_{DA} is affected by spin dynamics, the distance between the D and A, and orbital overlap of the D and A as well as the chromophore (C).^{3,17} Finally, the temperature and solvent system influence the k_{et} as well.^{3,17} However, the contributions of these factors are not as widely applicable as ΔG° so they will mainly be discussed where appropriate.

The following discussion will focus on the nonlinear dependence of the k_{et} on ΔG° . The mathematical relationship in eq 1 shows that as ΔG° changes three distinct regions of k_{et} dependence emerge. As ΔG° increases to the point where $\lambda = -\Delta G^\circ$, the k_{et} increases as well, which is called Marcus normal behavior.^{3,7,8,17-19} Marcus normal behavior is due to increasingly favorable overlap of the nuclear wavefunctions of the product and the reactant vibronic states as shown in Figure 2.¹⁷⁻¹⁹ At the point where $\lambda = -\Delta G^\circ$, the nuclear wavefunction overlap is maximized

for nuclear tunneling, which creates optimal electron transport conditions (Figure 2).¹⁷⁻¹⁹ If ΔG° increases past $\lambda = -\Delta G^\circ$, then the k_{et} should decrease, which is called Marcus inverted behavior.^{3,7-9,17-19} This effect is due to increasing exothermicity from a greater negative value of ΔG° causing unfavorable nuclear wavefunction overlap, which is often referred to as an unfavorable Franck-Condon factor (Figure 2).¹⁷⁻¹⁹

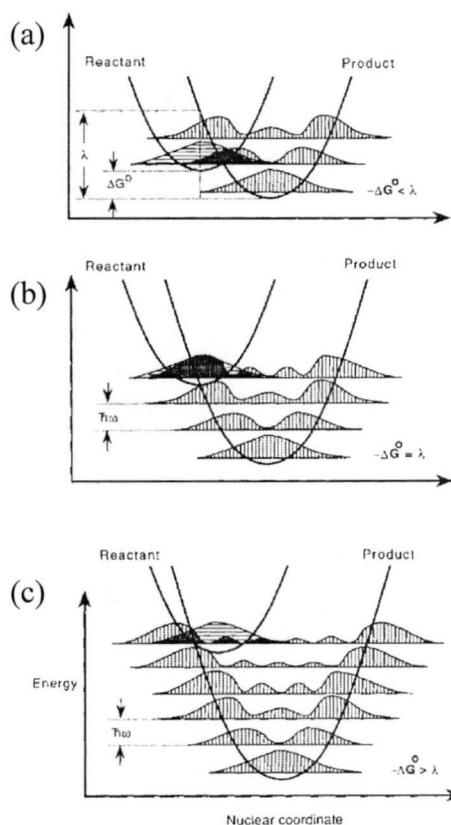


Figure 2. The dependence of the rate of electron transfer on the ΔG° of the reaction. (a) Marcus normal behavior (b) optimal for electron transfer due to enhanced nuclear tunneling and (c) Marcus inverted behavior. ΔG° is the thermodynamic driving force (free energy), ω is the frequency of the light, h is Planck's constant, and λ is the total reorganization energy. Adapted from ref 10.

Since the rate of CSS recombination has been shown to exhibit Marcus inverted behavior in many CSS complexes, this dependence on ΔG° has important implications.^{7,18,19} For most CSS complexes, the Marcus inverted behavior implies that increasing the driving force (ΔG°) of the reaction will hamper back electron transfer, thereby enhancing the quantum efficiency (Φ_{css}) and lifetime (τ_{css}) of the CSS and emission (τ_{em}).^{3,8,18} In the majority of D-C-A complexes this means that the structure of the D and A moieties of the CSS complexes can be altered to increase ΔG° .^{3,8,17-19} Structural alteration is a widely used approach and has been successful for increasing the Φ_{css} for many porphyrin and fullerene-type D-C-A studies.^{3,7,8,16-19} The D-C-A complexes of the type D-C²⁺-A²⁺ (with a Ru), on which the following discussion will focus, do exhibit Marcus normal and Marcus inverted behavior with respect to the rates of electron transfer.^{7,9,15} However, the Φ_{css} in these types of D-C²⁺-A²⁺ complexes is extremely high and does not seem to depend on driving force.^{7,9,16} This anomalous behavior was not well understood until recently, and may prove to be a great advantage for designing new charge-separated systems.¹⁶

The primary reason for this unusual behavior of the D-C²⁺-A²⁺ complexes is suggested to be the result of an intramolecular association prior to photoexcitation between the ML_x²⁺ and the donor moiety in the ground state.^{9,16} This will be referred to as the donor pre-association mechanism (DPA).

A significant amount of research on the D-C²⁺-A²⁺ complexes yielded important data that lead to the DPA mechanism. The most pertinent results will be outlined before discussing the details of the DPA mechanism.

Considering the reaction mechanism for D-C-A triads presented earlier in this paper, following initial photoexcitation to the ³MLCT state, intramolecular electron transfer causes that ³MLCT to be quenched.^{7,9-12,14,15} However, until the early 1990's it was not clear if the quenching step was by oxidative quenching, in which the acceptor is reduced, or reductive quenching, in which the donor is oxidized.^{11,16} By performing emission decay and time resolved absorption experiments on a series C²⁺-A²⁺ and D-C²⁺ diads (constructed to model the D-C²⁺-A²⁺ triads) the rates of oxidative ($k_{\text{et-ox}}$) and reductive quenching ($k_{\text{et-red}}$) could be extrapolated and compared.^{7,11,16} The series of C²⁺-A²⁺ and D-

C^{2+} diads had a variable number of methylene linkages between the bpy backbone and the DQ^{2+} or PTZ separately. By increasing the number of methylene linkages the reduction potential of the DQ^{2+} moiety could be altered (a longer methylene chain means that it is harder to reduce the DQ^{2+}), thereby influencing the ΔG° of formation for the CSS.^{7,11,16} This allowed for the direct comparison of ΔG° to the k_{et} .

These emission decay and time resolved absorption studies suggested that the k_{et-ox} and k_{et-red} quenching increased with ΔG° (i.e. the number of methylene linkages), which agrees with the predicted Marcus normal behavior.^{7,11,16} However, the k_{et-ox} for oxidative quenching was $2 \cdot 10^4$ times faster than the k_{et-red} for reductive quenching.^{7,11,16} Furthermore, it was found that the rate of emission decay (k_{emd}) of the $D-C^{2+}-A^{2+}$ triads follows the same trend as their parallel $C^{2+}-A^{2+}$ diads within a factor of 2, regardless of changes in the D moiety.^{7,11,16} Therefore, the initial step in forming a CSS in the $D-C^{2+}-A^{2+}$ complexes is suggested to be reduction of the acceptor by oxidative quenching.^{7,9,11,16} Magnetic Field Effect (MFE) studies at high fields ($B > 0.5$ T) also support that the initial quenching event is the reduction of the acceptor.¹⁴ Finally, the time resolved absorption studies indicated

that the kinetics of the initial quench is much slower than back electron transfer (k_{bet} , i.e. charge re-combination).^{7,9,11,15}

The results outlined above were interesting because the electron transfer in the $D-C^{2+}-A^{2+}$ systems exhibited an obvious dependence on the ΔG° of the system.^{7,9,11,12,15,16} However, the Φ_{css} did not seem to be greatly affected by the ΔG° , which contrasts with traditional Marcus theoretical predictions.^{9,13,14,16} These unusual results initiated studies on the other factors that could affect the Φ_{css} and enabled the elucidation of the donor pre-association mechanism (DPA). Therefore, the two main goals of these studies were: (1) explain how a CSS is formed with excellent Φ_{css} in complexes with extremely fast k_{bet} and (2) explain why the Φ_{css} does not depend on ΔG° . Logically, there is one explanation for the formation of the CSS in the $D-C^{2+}-A^{2+}$ complexes. After the initial reduction of the acceptor, the k_{cs} for formation of the charge-separated state (donor oxidation) must be faster than k_{bet} . However, just knowing that k_{cs} must be greater than k_{bet} does not elucidate the mechanistic details that cause k_{cs} to be so fast.^{7,9,16}

Two possible reaction mechanisms, diffusion-controlled bimolecular collision (BMC) and donor pre-association, were

proposed that could enhance the k_{cs} and are shown in Figure 3.¹⁶ In order to determine which reaction mechanism is responsible for the enhanced Φ_{css} the concentration of C and D were varied and several analytical methods were used to interpret the results. A bi-molecular $D/C^{2+}-A^{2+}$ CSS system was used so that the relative concentrations could be varied.^{9,16}

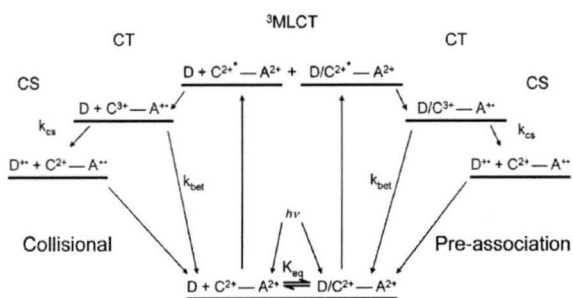


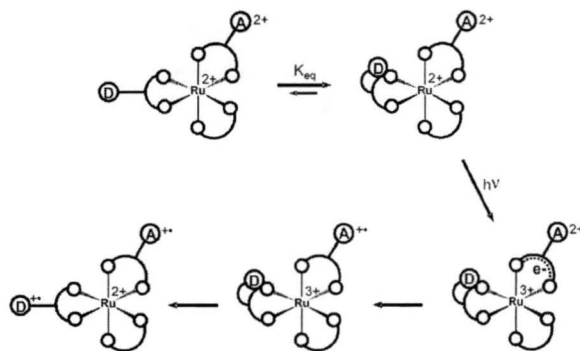
Figure 3. The two proposed mechanistic pathways for the formation of a CSS in the $D/C^{2+}-A^{2+}$ model compound. Reproduced from ref 16.

Transient absorption studies of the complex at varying D concentration allowed for kinetic modeling of both the BMC and DPA mechanistic cases. Using the transient absorption measurements k_{cs} , and k_{bet} were calculated. The calculated rate constant values were found to be more consistent with the DPA mechanism.¹⁶ More transient absorption measurements were taken of the $D/C^{2+}-A^{2+}$ compound in a solvent of sequentially varied viscosity. These measurements were intended to determine if the rate of diffusion would affect the Φ_{css} .

No effective change in the absorbance was detected even with a 25-fold increase in viscosity.¹⁶ This result was interpreted as evidence that the BMC mechanism is not responsible for the formation of the CSS.¹⁶

Although there is sufficient disproof of the BMC mechanism, the positive proof of the DPA mechanism was required. UV-spectra, time resolved emission decay, H^1 NMR, and 2D H^1 Roesy NMR data all suggested the DPA mechanism.¹⁶ These studies also indicated that the association is an intramolecular van der Waals interaction.¹⁶ The studies suggest that the association occurs prior to photoexcitation and broken immediately after donor oxidation due to electrostatic repulsion of positive charges as shown in Scheme 1.¹⁶

Scheme 1. The donor pre-association mechanism is seemingly responsible for the increased k_{cs} and Φ_{css} in the $D-C^{2+}-A^{2+}$ triads. This association between the D and the C^{2+} occurs prior to photoexcitation and is disassociated immediately after the donor is oxidized.



The elucidation of this mechanism is important for several reasons. First, it is suggested that the D/C²⁺ orbit coupling is enhanced by this associative interaction, which implies that orbit coupling influences the rates of electron transfer in the D-C-A complexes.¹⁶ Electron transfer in D-C-A diads/triads generally elicits very little change in the orbital coupling of the D and A moieties since there is little variation in their respective orientations.¹⁶ Therefore the rates of forward and back electron transfer are usually very similar. Increasing ΔG° helps break the competition between forward and back electron transfer in normal D-C-A complexes, which influences the Φ_{css} .¹⁶ Since the orbital coupling is enhanced in the D-C²⁺-A²⁺ complexes for only part of the DPA mechanism, the k_{cs} is increased for forward electron transfer.¹⁶ However, immediately after donor oxidation the orbital coupling is broken due to electrostatic repulsion, which would hamper the k_{bec} .¹⁶ The decrease in k_{bec} means that it is not necessary to increase the ΔG° to improve the Φ_{css} because nearly all of the CSS energy is retained and not lost to back electron transfer.¹⁶ A final important implication of the DPA is the ability to use the DPA as a tool for successful design of

new and more efficient D-C²⁺-A²⁺ type complexes.

Although the class of D-C²⁺-A²⁺ triads has been shown to have excellent values of Φ_{css} , the τ_{css} of the CSS is still not optimal. A longer τ_{css} for CSS complexes means that there is more time for effective utilization of the inherent chemical potential. Therefore, there is a need to figure out ways to enhance the τ_{css} . In past studies, the kinetics of formation of the CSS in natural systems has been shown to have a magnetic field dependence.¹⁴ Therefore, Magnetic Field Effect (MFE) studies on the transient absorbance of a series of D-C²⁺-A²⁺ triads were performed in order to determine the influence of a magnetic field on the lifetime of the CSS.^{13,14,16}

As mentioned previously these D-C²⁺-A²⁺ type complexes form a di-radical charge separated state (CSS). When the D moiety is PTZ the MFE studies suggest that the di-radical CSS is formed through a mechanism having the specific spin chemical dynamics outlined below. First, photoinitiated excitation promotes the Ru(II) from a singlet ground state to a singlet MLCT state, which undergoes rapid intersystem crossing to the triplet MLCT state.^{9,14,20} Then two spin-allowed electron transfers occur (reduction of the acceptor followed by oxidation of the

donor) to form a triplet di-radical charge separated spin state (^3CS).^{9,14,20} The CSS di-radical then decays back to the singlet ground state.^{9,14,20} Since CSS recombination has to occur from the triplet CSS state to the singlet ground state, CSS recombination (k_s) is formally spin forbidden.^{9,14,20} However, isotropic hyperfine coupling of the nearly degenerate singlet CSS (^1CS) and triplet CSS (^3CS) at zero field causes efficient mixing of the triplet and singlet states.^{9,14,20} Mixing of the singlet and triplet state allows for fast $^3\text{CS}/^1\text{CS}$ spin equilibration (k_{s,T_0}) making CSS recombination (k_s) a very rapid process.^{9,14,20} At zero field, the lifetime of the CSS state for the $\text{D-C}^{2+}\text{-A}^{2+}$ complexes studied was only measured to be between 100-300 ns.^{14,20} When a magnetic field between $0 \leq 0.5$ T was applied, the lifetime of the CSS increased by 7-12* the original value.^{9,14,20} A very small degree of structural dependence was also observed.^{9,14,20} The magnetic field dependence of the CSS lifetime is primarily due to the Zeeman splitting of the ^3CS energy levels as shown in Figure 4.^{9,14,20} The observed Zeeman splitting decreases the degree of isotropic hyperfine coupling of the ^1CS state and T^\pmCS states thereby slowing the rate of overall

* There was only one notable exception in which the lifetime of the CSS increased by a factor of 2.5.¹⁴

recombination.^{9,14,20} The Zeeman splitting also causes the kinetics of recombination to change from monoexponential at zero field to biexponential (with a fast and slow kinetic component) at an applied field.^{9,14,20} The fast component was shown to be the field independent T_0 recombination path (k_s), and the slow component was shown to be the field dependent T_\pm recombination path.^{9,14,20} The lifetime of the slow component is what is reported since it represents the lifetime of the CSS. It has been suggested that quantitative explanation and modeling of the $\text{D-C}^{2+}\text{-A}^{2+}$ triads decay kinetics can be described by the Hayashi and Nagakura *relaxation mechanism*.^{9,14,20}

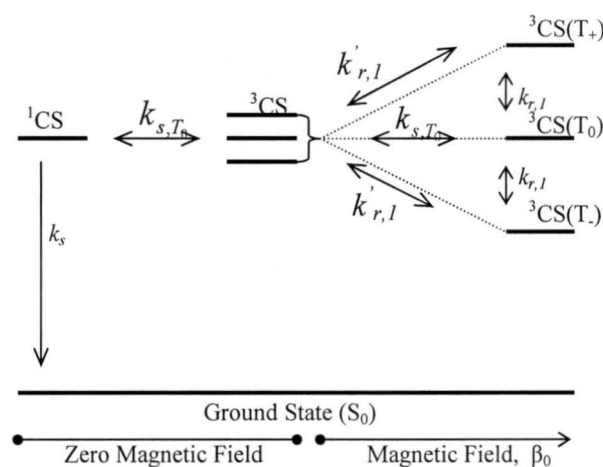


Figure 4. The Zeeman splitting of the ^3CS state in the presence of a magnetic field causes the kinetics of CSS recombination to change. This is due to the reduced isotropic coupling of the ^1CS and ^3CS states. The result is longer CSS lifetimes in the presence of a magnetic field. Adapted from ref 20.

Given that the magnetic fields necessary to significantly improve the CSS lifetime in the D-C²⁺-A²⁺ triads can be achieved with a handful of refrigerator magnets[‡], these are exciting results.²¹ It is definitely conceivable that small magnetic fields could be very useful for designing new systems that utilize photochemical energy, such as solar cells or water splitting devices.¹⁴

The previous studies indicate that two of the most important components to an efficient CSS, Φ_{CSS} and τ_{CSS} , are easily achieved in the D-C²⁺-A²⁺ complexes. The challenge is to further improve these complexes by accomplishing as good or better CSS properties in similar species made with different materials.

Although these CSS complexes may be getting extra attention in the past few years since the push for alternative energy and clean fuel sources has finally entered the mainstream, scientists have been fascinated with the topic for many decades. The incredible applications as well as the ability to mimic one of earth's most essential processes makes work on these types of complexes captivating, rewarding, and exciting as a field of study. There is a myriad of research available that reveal

[‡] The magnetic field of a normal refrigerator magnet is 5 mT.²¹

interesting aspects of the chemistry involved in the formation and utilization of the highly complex CSS species. Unfortunately, the background provided in this paper must be limited to the essential information necessary to understand the scope of the research describe herein. Therefore, the focus of this paper will now switch to the specific details of past projects leading up to, and the inspiration and for design this specific research project.

Project Rational and Design

It is easy to see why the D-C²⁺-A²⁺ type CSS complexes are exciting for new applications due to their intense absorption and unique ability to achieve high Φ_{CSS} and τ .⁹ These systems also have been shown to have favorable redox properties in solution.⁹ However, there are still a few drawbacks to the previously discussed systems. The experimental details provided in the preceding section were all from studies utilizing a Ru(II) chromophore.^{7,9-16,20} Other chromophores used for this type of D-C-A complex are Os, Re, and Pt.⁹ The rare and expensive nature of the metals typically used in D-C-A's is an obvious pitfall.⁹ Therefore, using the aforementioned metals does not really help the problem of making affordable D-C-A materials for applications such as

solar cells. The other porphyrin based D-C-A complexes also have their share of problems, such as synthetic complexity and unpredictable values of Φ and τ .^{3,8,9,18} It has become apparent to many in the scientific community that an alternative chromophore is needed to make these D-C²⁺-A²⁺ type complexes useful and reasonable for real applications. One alternative system that seems to exhibit promising properties is Cu(phen)₂⁺, in which phen is a 2,9-disubstituted-1,10-phenanthroline.^{9,22-36}

Although Cu(I) complexes of the type Cu(phen)₂⁺ have shown potential applicability, there are also drawbacks associated with complexes based on Cu(I).⁹ Cu(I) has been the subject of CSS studies since the late 1970's. At first, Cu(I) did not seem as reasonable as the Ru(II) analogs due to its lack of emission in solution.^{27,28,31,34,35} However, it has been established in a number of studies that Cu(I) complexes do demonstrate strong, broad photoexcitation to a visible MLCT state with unsubstituted phen and bpy ligands.^{9,28,35} Excitation in the Cu(I) complexes is analogous to the Ru(II) complexes: photoexcitation to the singlet ¹MLCT, which converts rapidly to the ³MLCT via an intersystem crossing mechanism.^{9,20,28} However the difference in energy between the singlet and triplet

MLCT states in the Cu(I) complexes has been suggested to be smaller than in the Ru(II) analogs.^{9,28} This difference in ¹MLCT/³MLCT state energies could imply that the Φ_{CSS} will exhibit enhanced MFE's.^{9,28} As mentioned previously, these unsubstituted complexes are non-emissive in solution, even when the solvent is non-coordinating (coordinating solvents can quench the emission process).^{9,27,28,37} This is important because it lead researchers to investigate the mechanism of emissive quenching in the Cu(I) complexes.

The photophysical behavior of the Cu(I) complexes has been studied quite extensively in order to rationalize the emission quenching process in solution.^{24,34,38} Several studies suggest that the emission quenching behavior is primarily caused by the Jahn Teller distortion inherent in the d⁹ Cu(II) excited MLCT state.^{9,38-40} This distortion from the Franck-Condon MLCT tetrahedral geometry toward square planar is suggested to be very rapid and accompanied by the coordination of a solvent or anion, which is suggested to be the formation of an exciplex as shown in Figure 5.^{4,9,32,34,36,38-40} Kinetic studies on exciplexes have shown that non-radiative decay occurs immediately following the coordination of the solvent /anion.^{38,40}

Therefore, it is logical to assume that if bulky substituents are placed on the 2,9 positions of the 1,10 phenanthrolines, the increased steric hindrance could have two positive effects: reduce the amount of distortion from the tetrahedral to square planar geometry and crowd the metal center, inhibiting solvent/anion coordination. Several studies have recorded emission from Cu(I) complexes in solution if bulky enough substituents are in the 2,9 positions.^{9,32,34,35} The induced stabilization of the Cu^I complexes due to bulky substituents has also been shown to influence redox potential of the Cu^I/Cu^{II}.³² This indicates that the redox potential could be easily tuned by the proper selection of bulky substituent.

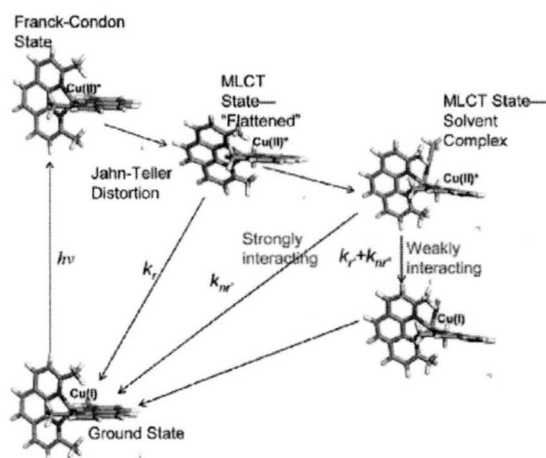


Figure 5. The mechanism of emission quenching in the Cu(I) complexes is suggested to be due to the Jahn-Teller distortion of the d^9 Cu(II)* excited state followed by coordination by solvent or counterion. Reproduced from ref 37.

When bulky substituents are substituted on the 2,9 positions of the phen moieties the lability of the ligands in Cu(I)(phen)₂ complexes can be a problem.⁹ The inherent lability of Cu(I) complexes has been a significant hindrance to the fabrication and isolation of many heteroleptic Cu(I) complexes in the past due to fast ligand exchange back to a mono-phen analog.^{9,41} However, studies on Cu(I) phenanthroline complexes with bulky substituents in the 2,9 positions have indicated that the formation of the bis-complex could be related to two factors: (1) the size of the substituents due to steric hindrance in the Cu(I) coordination sphere, (2) and the binding constant of the second phen ligand.^{9,41} The binding constant of the second ligand could also be influenced by the steric environment imposed by the first phen ligand.^{9,41} Therefore, it could be possible to utilize this inherent lability as a self-assembly mechanism for the formation of a Donor-Chromophore-Acceptor type complex.

If a phen ligand with the bulky groups substituted in the 2,9 positions is fabricated as a chloro complex with Cu(I) to make Cu(I)(2,9-bulky-phen)Cl, then the binding constant of a second less bulky phen moiety should be reasonable. Furthermore, due to the chelate effect, the formation of the bis-

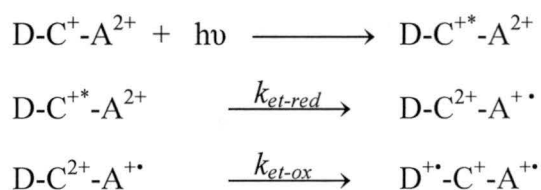
phen complex should be favored to the mono-phen, mono-chloro complex.⁹ This type of reaction scheme has been preceded in the literature.^{25,26,33} Simple molecular dynamics (MD) calculations were performed that also indicated the validity of this type of reaction scheme.⁹ Specifically, the MD calculations indicated that formation of the $[\text{Cu}(\text{bPZmp})(\text{dmp})]^+$ complex was much more enthalpically favored than the $[(\text{bPZmp})_2\text{Cu}]^+$ complex due to the reduced strain energy (bPZmp= 2,9- bis((pheno-thiazine)methyl)-1,10-phenanthroline; dmp= 2,9-dimethyl-1,10-phenanthroline).⁹

Having briefly outlined the background research relevant to this project, the major objectives and design aspects will now be discussed. Attention will be given to the aspects of design that will be attempted in order to circumvent previously obstacles inherent in the project.

The major goal of this project is to try to fabricate a heteroleptic, Cu(I) containing complex capable of achieving a CSS similar to the Ru(II) analogs.⁹ The proposed reactions scheme for the Cu(I) complexes is shown in Scheme 2. When designing a Cu(I) complex for the formation of a CSS several factors must be considered that did not necessarily apply to the parallel Ru(II) complexes. The major things to consider in

the design process are as follows: the DPA mechanism of charge separation, bulkiness of substituents on the phen D and phen A, and finally the redox properties of the D and A.

Scheme 2. The proposed series of reactions that lead to the CSS with the Cu(I) complexes. Reproduced from ref 9.



Assuming that the Cu(I) complexes will act similarly to the other D-C-A complexes with metal chromophores, the DPA mechanism will result in a high values of Φ_{css} . However, in order to facilitate the DPA mechanism, the linkages between the D and the phen ligand must be long enough and flexible. If the linkages are not long or flexible enough to allow the necessary spin-orbit coupling that occurs between D and phen, the Φ_{css} will be hindered.

The bulkiness of the D and A moieties also play an important role in the design of this novel Cu(I) complex. One of the phen ligands must have bulky ligands on the 2,9 positions of the phen and the other must not be bulky. This type of setup will allow for the self-assembly of the heteroleptic complex as previously described. Theoretically, this will also crowd the Cu(I)

potential of PTZ, switching to phenoxazine (POZ) (R-POZ, $E_{1/2}=0.6V$), or using a modified POZ.^{9,25}

Finally, the last problem that could occur is a problem that exists in all forms of experimental research. The Cu^I complex could seem perfect yet not display any of the chemistry for which it was originally devised, i.e. formation of a CSS. In this case, further evaluation will be necessary.

The first challenge in this project is the synthesis of the D, A and D-C-A moieties. Synthesis of the individual components was expected to be easy, however, this step has proven to be more difficult than initially anticipated.

Experimental

The 1H NMR spectra were obtained on a Varian Inova 300 MHz (VI300), Varian Mercury-Inova 300 MHz (VMI300), or Varian Inova 400 MHz (VI400) machine. All mass spectrometry was performed by the CIF using either electrospray ionization, or atmospheric pressure chemical ionization time-of-flight (ES/APCI TOF) for samples with some polarity. Fast atom bombardment, or electron ionization with 70 eV electrons was used for non-polar samples. IR spectrometry was performed on an Avatar 320 FT-IR of Nicolet Instrument

Corp. along with the EZ Omnic E.S.P. v.5.2 software. All chemicals used in these experiments are listed in Section 1 of the Supplemental Information.

Literature methods were used for the preparation of 2,9-bis(trichloromethyl)-1,10-phenanthroline, 2,9-bis(methoxycarbonyl)-1,10-phenanthroline, 2,9-bis(hydroxymethyl)-1,10-phenanthroline, 2,9-bis(chloromethyl)-1,10-phenanthroline, 2,9-bis(bromomethyl)-1,10-phenanthroline, and 2,9-bis[(*tert*-butyldimethylsilyl)-methyl]-1,10-phenanthroline.⁴³⁻⁴⁶ All changes made to the literature methods used to prepare these compounds are detailed in the Supplemental Information, Section 1, Reactions I-III B.

2,9-bis[(phenoxazine)methyl]-1,10-phenanthroline (bPOmp). Glassware was stored in an oven at 250 °C for at least 1 hr, flamed and degassed under Ar until cool. 2,9-bis(chloromethyl)-1,10-phenanthroline (cmp) was stored in a desiccator overnight. Dry toluene solvent was obtained from the Williams' lab solvent system. Cmp (0.0214 g, 0.0772 mmol) and phenoxazine (POZ, 0.0406 g, 0.2150 mmol) were dissolved in approximately 10 mL dry toluene in a 3-neck round-bottom flask) and put under Ar (molar ratio of approx. 1 cmp: 3 POZ). One microspatula tip-full of potassium *tert*-

butoxide was added to the reaction mixture and was sonicated. The reaction mixture slowly turned light red. More potassium *tert*-butoxide was added in intervals by the microspatula tip-full and followed by TLC (30% ethyl acetate: 70% hexanes). The color of the reaction turns dark, being cherry red when the reaction is complete. The reaction was quenched with glacial acetic acid. Water was added and the product was extracted with chloroform (3x). The product was suspended/dissolved in hot hexanes, put in the freezer and the ppt filtered off and dried in the vacuum oven. Products purified by column chromatography (10% hexanes: 2% EtOAc: 88% CH₂Cl₂). The column was flushed with hexanes containing 3 drops of triethylamine, and then flushed with hexanes. The product was then recrystallized from CHCl₃/MeOH. A small amount of impurity was still indicated by TLC and ¹H NMR, so further purification is necessary. The product was an orange/yellow solid. An ¹H NMR (300 MHz) was taken of the impure product and is shown in the Supplemental Information, Section 2: Reaction VI.

All of the experiments that were attempted in order to synthesize bPOmp unsuccessfully are detailed in the Supplemental Information. The important

results from these unsuccessful attempts will be discussed in the Results and Discussion and referenced to the appropriate section in the Supplemental Information, Section 2: Reaction IV-V.

Results and Discussion

The synthetic approaches chosen for the preparation of the proposed D-C-A triad were chosen based on their literature precedence and simplicity. However, synthesis of just the Donor moiety has proven a non-trivial task. Making the donor requires making either the cmp or bmp ligand and synthesizing these ligands is often a very time-consuming, multistep process, with a lot of necessary purification. The two most accepted synthetic methods are more than twenty-five years old and have proven to be quite inefficient.^{43,46} Although these papers report excellent yields for each synthetic step, the experimentally derived yields seem to deviate greatly even after several attempts (See Supplemental Information, Section 1: Reaction II).

A new approach to the synthesis of the starting materials cmp and dmp was found in the literature, which has significantly sped up the synthetic process.^{44,45} This new process involves two steps, the reported

yields are experimentally attainable, and the products are easily purified (See Supplemental Information, Section 1: Reaction IIIA and IIIB). These two synthetic processes are very similar to the first synthetic scheme that was tried in which the synthesis of 2,9-Bis[(trimethylsilyl)methyl]-1,10-phenanthroline (bTMSp) was attempted. In these two syntheses, the 2,9-bis[(*tert*-butyldimethylsilyl)methyl]-1,10-phenanthroline (bTBSp) and the 2,9-bis[(triethylsilyl)methyl]-1,10-phenanthroline (bTESp) products are synthesized. A possible pattern emerged in the literature about these syntheses that offers insight into why the bTBSp and bTESp are easily prepared yet bTMSp is not. The reported yields for the synthesis of bTBSp and bTESp were 98% and 84% separately. Although almost identical procedures were used to synthesize the bTMSp, no product was formed.⁴⁷ This suggests that the bulkiness of the silyl group influences the reactivity. The greater electron donating character of the triethylsilyl and *tert*-butyldimethyl groups could be activating the Si-Cl bond of the triethylsilyl chloride and *tert*-butyldimethylsilyl chloride, enhancing the reactivity.⁴⁸

The conversion of bTMSp to cmp or bmp is relatively straightforward, and

although this has only been attempted twice, an overall yield of 30.77% has been achieved. Considering that the best yield achieved from the old procedures^{43,46} was about 13.70% (literature reports 51.33%), this is a great improvement. However, the literature suggests by using bTESp and converting it to bmp better yields (~60%) can be obtained.⁴⁴ More work is needed in order to figure out how to increase the yield of the starting material.

The synthetic strategies used to attach the PXZ to 2,9-methyl position of the cmp and bmp seem very viable (See Supplemental Information, Section 2: Reaction IV). These methods have been very successful for analogous bipyridine syntheses and were therefore, the first approach taken for the synthesis of bPZmp.

As can be seen from Section 2: Table IVA in the Supplemental Information, many different approaches were taken to force the reaction. However, no appreciable amount of product was obtained. No significant clues or patterns emerged from the ¹H NMR or TLC data that would give insight into the problem until Trial 6. In this trial the mass spec data was clean enough to pick out and analyze the relevant peaks. It was determined that many of the m/z peaks corresponded to ethoxymethyl substituted

phenanthrolines. This suggests that there is little to no reaction occurring between the dmp and deprotonated PTZ. Also, the presence of the ethoxy-substituted dmp's suggests that the EtOH quenching reagent is a better nucleophile for this reaction than the deprotonated PTZ. To test this idea, the reaction in Trial 7 was quenched with glacial acetic acid due to the poor nucleophilicity of the acetate anion. The mass spec results of Trial 7 did not include as many peaks corresponding the acetate-substituted complex. However, this could also merely reflect the ability of the acetate-substituted complexes to form an ion.

It was also noticed that the mass spec for Trials 5-7 had sodium or lithium coordination complexes. Although this seems obvious since NaH or n-butyl lithium (n-BL) were used to deprotonate PTZ, this was an important realization. Coordination of lithium to the cmp or bmp has been known to activate the 2,9 methylene proton, which could then reprotonate the PTZ.⁴⁸ This reprotonation would not only annul the reactivity of the PTZ, but also the cmp or bmp.⁴⁸

Several methods were devised in order to avoid interference in the reaction by sodium or lithium coordination: include 12-crown-4 or 15-crown-6 to selectively

sequester the Li⁺ and Na⁺ ions, use a more coordinating solvent to compete for coordination sites, use potassium *tert*-butoxide (K-tB) since K⁺ is larger and therefore less coordinating with phen. At this time a new paper was found where PTZ groups were successfully attached to 3,8-dibromo-1,10-phenanthroline using a Pd(0) catalyst and chelating phosphine ligands.⁴⁹

This new Pd catalyzed approach was attempted on a small scale in toluene. POZ was used instead of PTZ in this case as well due to enhanced reactivity.⁴⁸ Sodium carbonate was used as the base at first, but TLC showed that the reaction was not proceeding, even when heated to ~80 ° C. When K-tB was added the solution immediately changed color, and TLC indicated that a reaction was occurring. ¹H NMR (VI400) and mass spec verified the product of this reaction as bPOmp.

In order to determine if the Pd(0) catalyst was needed the reaction was repeated in a coordinating solvent, with POZ, and using K-tB. The reaction was retried in the absence of the Pd(0) catalyst, TPP, and Na₂CO₃. This reaction also yielded bPOmp as verified by ¹H NMR (VI300) and mass spec. These results indicated that the coordination of Na⁺, and Li⁺ might have been interfering with the

reactivity of the PTZ by activating the methylene protons on the cmp or bmp. These data also indicate that the Pd(0) catalyst is not required for this reaction to proceed. Since both the trials for this reaction were performed on such a small scale, they were combined for purification and therefore an accurate yield cannot be reported at this time. This reaction reported in the experimental section.

Conclusions

As can be seen from the previous discussion most of the experimental work done on this project has been synthesis of the Donor. However, several important observations about these syntheses have been made, which can be very helpful for similar procedures in the future. First, the reactivity of phen ligands does not always parallel the bpy analogs. Although the two structures seem similar and exhibit similar properties in D-C-A triads, their reactivity is inherently different.

Based on the previous experiments it seems that this difference in reactivity is primarily due to the rigid -planar structure. Since the bpy has the ability to rotate freely about the center, the two nitrogen atoms are not always aligned for strong coordination interactions in solution. This could be an

explanation for why free ions in solution do not hinder reactions involving bpy as much as phen.

The rigid-planar structure is also why phen seems viable in the proposed D-C-A triad. The static, constant steric hindrance imposed by the large methyl-POZ moieties at the 2,9 position of a rigid 1,10 phenanthroline could provide excellent stabilization for the Cu (I) against Jahn-Teller distortion.⁹ The planarity inherent in the phenanthroline structure could also help lock the A moiety around the Cu (I) center by possible π -stacking interactions with the POZ substituents.⁴⁸

In addition, using POZ attached to a flexible methylene linkage should enable the D/C interactions necessary for the DPA mechanism and favorable redox properties for the formation of a CSS.⁹ Finally, the energy difference between the ¹MLCT and the ³MLCT states in Cu(I) D-C-A complexes are suggested to be smaller than Ru(II), possibly enabling a longer, more efficient CSS in smaller magnetic fields.⁹

Future Work

This project is infused with future work, therefore short-term future work goals and will be discussed first and then long-term goals. The main short-term future work

goals are to try to improve the yields in the synthesis of cmp and bmp. The first way that will be tried for improving the yield of cmp or bmp will be utilizing bTESp (instead of bTBSp) for the preparation of cmp and bmp according to the literature procedure.⁴⁴ Another short-term goal is to attempt to synthesize bPZmp by non-Pd(0) synthetic methods, just for proof of concept. The non-Pd(0) reaction should also be attempted using n-BL and a coordinating solvent. This would help elucidate if K-tB is needed or if a coordinating solvent is enough for the synthesis of bPZmp/bPOmp. A final short-term goal is to successfully synthesize the A moiety using literature procedures.⁵⁰⁻⁵⁴

One of the long-term goals of this project is to try to get the triad to self assemble in solution and follow the process by ¹H NMR. After the assembly of the D-C-A triad has been confirmed, electrochemical measurements will be taken in order to determine if the A can be reduced by the Cu(I)^{*} and the D can be oxidized by Cu(II). If the redox reactions are not occurring then the D and A moieties will be modified in order to try to tune the E_{1/2}. If the redox chemistry is appropriate then transient absorption and MFE measurements will be performed in order to determine if a CSS is

formed. A final goal is to try to enhance the Φ_{CSS} and τ_{CSS} by structural modification.

References

- (1) Bassham, J. A.; Benson, A. A.; Calvin, M. *J. Biol. Chem.* **1950**, *185*, 781-787.
- (2) Dismukes, G. C. *Science* **2001**, *292*, 447-448.
- (3) Wasielewski, M. R. *J. Org. Chem.* **2006**, *71*, 5051-5066.
- (4) Barber, J.; Andersson, B. *Nature* **1994**, *370*, 31-34.
- (5) Bolton, J. R.; Strickler, S. J.; Connolly, J. S. *Nature* **1985**, *316*, 495-500.
- (6) O'Regan, B.; Gratzel, M. *Nature* **1991**, *353*, 737-739.
- (7) Larson, S. L.; Elliott, C. M.; Kelley, D. F. *J. Phys. Chem.* **1995**, *99*, 6530-6539.
- (8) Gust, D.; Moore, T. A. *Science* **1989**, *244*, 35-41.
- (9) Elliott, C. M.; Steiner, U. E.; Szamel, G.; Department of Energy Grant Number: DE-FG02-04ER15591; Department of Chemistry, Colorado State University, Fort Collins, CO 80523.
- (10) Cooley, L. F.; Headford, C. E. L.; Elliott, C. M.; Kelley, D. F. *J. Am. Chem. Soc.* **1988**, *110*, 6673-6682.
- (11) Cooley, L. F.; Larson, S. L.; Elliott, C. M.; Kelley, D. F. *J. Phys. Chem.* **1991**, *95*, 10694-10700.
- (12) Elliott, C. M.; Freitag, R. A.; Blaney, D. D. *J. Am. Chem. Soc.* **1985**, *107*, 4647-4655.
- (13) Klumpp, T.; Linsenmann, M.; Larson, S. L.; Limoges, B. R.; Buerstner, D.; Krissinel, E. B.; Elliott, C. M.; Steiner, U. E. *J. Am. Chem. Soc.* **1999**, *121*, 4092.
- (14) Klumpp, T.; Linsenmann, M.; Larson, S. L.; Limoges, B. R.; Buerstner, D.; Krissinel, E. B.; Elliott, C. M.; Steiner, U. E. *J. Am. Chem. Soc.* **1999**, *121*, 1076-1087.

- (15) Larson, S. L.; Cooley, L. F.; Elliott, C. M.; Kelley, D. F. *J. Am. Chem. Soc.* **1992**, *114*, 9504-9509.
- (16) Weber, J. M.; Rawls, M. T.; MacKenzie, V. J.; Limoges, B. R.; Elliott, C. M. *J. Am. Chem. Soc.* **2007**, *129*, 313-320.
- (17) Moser, C. C.; Keske, J. M.; Warncke, K.; Farid, R. S.; Dutton, P. L. *Nature* **1992**, *355*, 796-802.
- (18) Wasielewski, M. R.; Niemczyk, M. P.; Szec, W. A.; Pewitt, E. B. *J. Am. Chem. Soc.* **1985**, *107*, 1080-1082.
- (19) Williams, R. M. Introduction to Electron Transfer. [http://www.home.uva.nl/r.m.williams/Introduction to ET-30.htm](http://www.home.uva.nl/r.m.williams/Introduction%20to%20ET-30.htm) (accessed Aug 2008) Universiteit van Amsterdam: Amsterdam, 2007, p28.
- (20) Rawls, M. T.; Kollmannsberger, G.; Elliott, C. M.; Steiner, U. E. *J. Phys. Chem. A* **2007**, *111*, 3485-3496.
- (21) Nevus Network. Information on MRI Technique. <http://www.nevusnetwork.org/mritech.htm> (accessed Aug 2008)
- (22) Blaskie, M. W.; McMillin, D. R. *Inorg. Chem.* **1980**, *19*, 3519-3522.
- (23) Casadonte, D. J.; McMillin, D. R. *Inorg. Chem.* **1987**, *26*, 3950.
- (24) Cunningham, C. T.; Cunningham, K. L. H.; Michalec, J. F.; McMillin, D. R. *Inorg. Chem.* **1999**, *38*, 4388-4392.
- (25) Cuttell, D. G.; Kuang, S.-M.; Fanwick, P. E.; McMillin, D. R.; Walton, R. A. *J. Am. Chem. Soc.* **2002**, *124*, 6-7.
- (26) Gandhi, B. A.; Green, O.; Burstyn, J. N. *Inorg. Chem.* **2007**, *46*, 3816-3825.
- (27) Ichinaga, A. K.; Kirchhoff, J. R.; McMillin, D. R.; Dietrich-Buchecker, C. O.; Marnot, P. A.; Sauvage, J. P. *Inorg. Chem.* **1987**, *26*, 4290-4292.
- (28) Kirchhoff, J. R.; Gamache, R. E.; Blaskie, M. W.; Paggio, A. A. D.; Lengel, R. K.; McMillin, D. R. *Inorg. Chem.* **1983**, *22*, 2380-2384.
- (29) Kovalevsky, A. Y.; Gembicky, M.; Coppens, P. *Inorg. Chem.* **2004**, *43*, 8282-8289.
- (30) Kuang, S.-M.; Cuttell, D. G.; McMillin, D. R.; Fanwick, P. E.; Walton, R. A. *Inorg. Chem.* **2002**, *41*, 3313-3322.
- (31) McMillin, D. R.; Buckner, M. T.; Ahn, B. T. *Inorg. Chem.* **1977**, *16*, 943-945.
- (32) Miller, M. T.; Gantzel, P. K.; Karpishin, T. B. *Angew. Chem. Int. Ed.* **1998**, *37*, 1556-1558.
- (33) Miller, M. T.; Gantzel, P. K.; Karpishin, T. B. *J. Am. Chem. Soc.* **1999**, *121*, 4292-4293.
- (34) Palmer, C. E. A.; McMillin, D. R. *Inorg. Chem.* **1987**, *26*, 3837-3840.
- (35) Rader, R. A.; McMillin, D. R.; Buckner, M. T.; Matthews, T. G.; Casadonte, D. J.; Lengel, R. K.; Whittaker, S. B.; Darmon, L. M.; Lytle, F. E. *J. Am. Chem. Soc.* **1981**, *103*, 5906-5912.
- (36) Ruthkosky, M.; Kelly, C. A.; Zaros, M. C.; Meyer, G. J. *J. Am. Chem. Soc.* **1997**, *119*, 12004-12005.
- (37) Dietrich-Buchecker, C. O.; Marnot, P. A.; Sauvage, J. P.; Kirchhoff, J. R.; McMillin, D. R. *J. Chem. Soc., Chem. Commun.* **1983**, *9*, 513-515.
- (38) Shaw, G. B.; Grant, C. D.; Shirota, H.; Castner Jr., E. W.; Meyer, G. J.; Chen, L. X. *J. Am. Chem. Soc.* **2007**, *129*, 2147.
- (39) McMillin, D. R.; Kirchhoff, J. R.; Goodwin, K. V. *Coord. Chem. Rev.* **1985**, *64*, 83-92.
- (40) Palmer, C. E. A.; McMillin, D. R.; Kirmaier, C.; Holton, D. *Inorg. Chem.* **1987**, *26*, 3167-3170.
- (41) Pallenberg, A. J.; Koenig, K. S.; Barnhart, D. M. *Inorg. Chem.* **1995**, *34*, 2833-2840.
- (42) Elliott, C. M.; Freitag, R. A. *J. Chem. Soc., Chem. Commun.* **1985**, 156-157.

- (43) Chandler, C. J.; Deady, L. W.; Reiss, J. *A. J. Heterocyclic Chem.* **1981**, *18*, 599-601.
- (44) Eggert, J. P. W.; Harrowfield, J.; Lüning, U.; Skelton, B. W.; White, A. H.; Löffler, F.; Konrad, S. *Eur. J. Org. Chem* **2005**, 1348-1353.
- (45) Eggert, J. P. W.; Lüning, U.; Näther, C. *Eur. J. Org. Chem* **2005**, 1107-1112.
- (46) Newkome, G. R.; Kiefer, G. E.; Puckett, W. E. Vreeland, T. *J. Org. Chem.* **1983**, *48*, 5112-5114.
- (47) Smith, A. P. Lamba, J. J. S.; Fraser, C. L. *Org. Synth.* **2002**, *78*, 82-87.
- (48) Elliott, C. M. Colorado State University, Fort Collins, CO. Personal Communication, 2008.
- (49) Suzuki, H.; Kanbara, T.; Yamamoto, T. *Inorg. Chim. Acta* **2004**, *357*, 4335-4340.
- (50) Dolman, N. P.; More, J. C. A.; Alt, A.; Knauss, J. L.; Troop, H. M.; Bleakman, D.; Collingridge, G. L.; Jane, D. E. *J. Med. Chem.* **2006**, *49*, 2579-2592.
- (51) Garas, A. M. S.; Vagg, R. S. *J. Heterocyclic Chem.* **2000**, *37*, 151-158.
- (52) Leblanc, Y.; Dufresne, C.; Carson, R.; Morency, L.; Welch, C. J. *Tetrahedron: Asymmetry* **2001**, *12*, 3063-3066.
- (53) Wu, J. Z.; Wang, L.; Yang, G.; Zeng, T. X.; L.N., J. *Chin. Chem. Lett* **1995**, *6*, 893-896.
- (54) Strazzolini, P.; Runcio, A. *Eur. J. Org. Chem* **2003**, 526-536.

Supplementary Information

Section I: Technical Information and Starting Material Synthesis Procedures

List of chemicals, suppliers and purities used in this research

(Note: - indicates that the information was not available or is not applicable)

Chemical Name	Company	Purity
1,2 dibromotetrafluoroethane	SynQuest Laboratories, Inc.	< 99%
2,9-dimethyl-1,10-phenanthroline (hemihydrate)	Lancaster Synthesis Ltd.	98%
4,4'-bipyridine (hydrate)	City Chemical Corp.	-
α,α' -dibromo-p-xylene	Aldrich	98%
aluminum oxide (activated basic, Brockmann I, standard grade 150 mesh, 58Å)	Sigma-Aldrich	-
acetic acid (Glacial)	Mallinckrodt Chemicals	99%
chlorotrimethylsilane (redistilled)	Aldrich	99%
Filter agent celite(545)	Aldrich	-
hexachloroethane	Aldrich	99%
hydrobromic acid (48% in water)	Acros Organics	-
hydrochloric acid (~37%)	Mallinckrodt Chemicals	-
n-butyl lithium (1.6 M in hexanes)	Acros Organics	-
n-butyl lithium (2.5 M in hexanes)	Acros Organics	-
phenothiazine	-	-
phenoxazine	Aldrich	97%
phosphorous trichloride	Aldrich	98%
silica gel (200-400 mesh, 60 Å) for column chromatography	Sigma-Aldrich	
sodium carbonate (anhydrous)	Fisher	100%
sodium hydride (60% dispersion in mineral oil)	Acros Organics	-
sodium hydride (dry, 97%)	Aldrich	97%
sulfuric acid (ACS)	EMD	95-98%
<i>tert</i> -butylchlorodimethyl silane	Acros Organics	98%
tetrakis(triphenylphosphine)Pd(0)	Aldrich	99%
triphenylphosphine	Aldrich	99%
uniplate silica gel gf- TLC plates (250 microns)	Analtech	-
Solvent Name	Company	Grade/Purity
acetonitrile	Fisher	99.90%
deuterated chloroform	Cambridge Isotope Laboratories	99.80%
dichloromethane (ACS)	Mallinckrodt Chemicals	99.50%
absolute ethanol, anhydrous (EtOH)-(ACS/USP)	Pharmaco- AAPER	200 proof
ethyl acetate (EtOAc)-(ACS)	Fisher	99.90%
ethyl ether (ACS)	Fisher	99.90%
hexanes (ACS)	Mallinckrodt Chemicals	98.50%
methanol (MeOH)- (ACS)	Fisher	99.9%
n-heptane	Fisher	HPLC
Tetrahydrofuran (THF)- (ACS)	Fisher	ACS
toluene (ACS)	Fisher	99.90%
Triethylamine (TEA)	Fisher	peptide synthesis

Comprehensive List of Attempted Syntheses for the 2,9-Bis(chloro or bromo)methyl)-1,10-Phenanthroline Starting Material

The list shown below is meant to give an overview on the many different procedures attempted in order to synthesize the starting material 2,9-bis[(chloro)methyl]-1,10-phenanthroline (cmp) or 2,9-bis[(bromo)methyl]-1,10-phenanthroline (bmp). All of the synthetic schemes were either directly from literature procedures or a modified version of a literature procedure. Therefore, the conditions and literature references (Lit Ref.) are listed so the reader can note the changes in procedure from the literature reference if any were made.

Reaction I (Lit ref: 47)

Scheme I



Table I: The calculations for the synthesis of 2,9-Bis(trimethylsilyl)methyl-1,10-phenanthroline.

Compound	Formula Weight (g/mol)	Density (g/ml)	Quantity	Mol	mmol
diisopropyl amine	101.19	0.722	2.0 mL	0.014	14.270
n-butyl lithium (1.6 M)	1.6 M	-	9.0 mL	0.014	14.400
2,9-dimethyl-1,10-phenanthroline (dmp)	208.26	-	1 g	0.005	4.802
trimethylsilyl chloride (TMSCl)	108.64	0.856	2.4 mL	0.019	18.910
2,9 bis(trimethylsilyl)methyl-1,10 phenanthroline (bTMSp)	352.62	-	-	-	-

Conditions: This reaction was performed under nitrogen. Deprotonation of diisopropyl amine (DiiA) was performed by dropwise addition of the n-butyl lithium (n-BL) in an ice bath (~ 0 °C) and run for 20 min to make lithium diisopropylamide (LDA). Dmp was dissolved in dry tetrahydrofuran (THF) and added to the LDA via cannula. The ice bath was replaced by a dry ice/acetone bath (~ -78 °C) and allowed to react for 1 hour. TMSCl was added and the reaction was quenched after 1 min. The product was rinsed with NaHCO₃ and allowed to come to room temperature (RT). Then the product was extracted with CH₂Cl₂, dried with Na₂SO₄, filtered, rotovapped, and characterized by ¹H NMR in CDCl₃ on the Varian-Mercury Innova 300 Mhz (VMI300).

Comments: The goal of this reaction was to convert the bTMSp into the cmp starting material. However, this reaction was attempted seven times with different reaction conditions, and did not yield the desired product. The alterations made for each different attempt are outlined below.

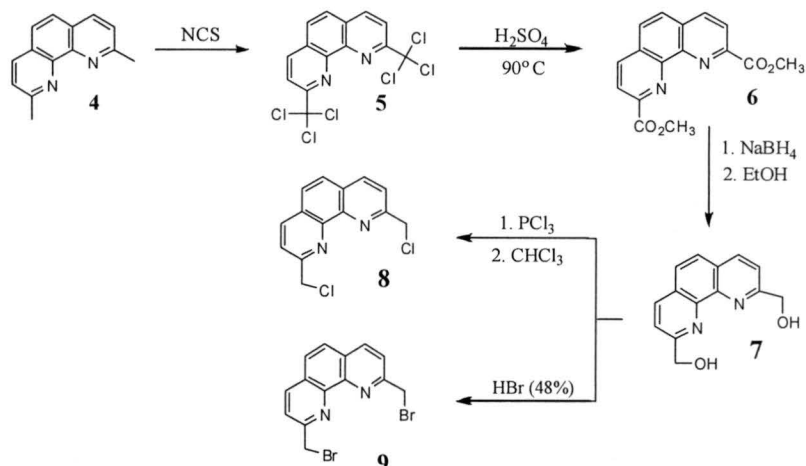
Table IA: Details of changes made to the synthesis shown in Scheme I.

Trial	Stoichiometry (dmp:LDA: TMSCl)	Conditions	Method of Characterization
1 (shown above)	(1: 3: 4)	Described above	¹ H nmr in CDCl ₃ on the VMI300
2	(1: 2.4: 2.5)	DiiA and n-BL were reacted for 30 min. After dmp was added, rxn was run for 30 min, After TMSCl was added, rxn run for 15 sec, then quenched.	¹ H nmr in CDCl ₃ on the VMI300 -TLC
3	(1: 2.5: 2)	DiiA and n-BL were reacted for 30 min. Dmp and LDA were reacted for 1.5 h. After TMSCl was added, rxn run for 15 sec, then quenched.	¹ H nmr in CDCl ₃ on the VMI300 -TLC
4	(1: 6: 2)	Rxn done under Ar. DiiA and n-BL were reacted for 30 min. When dmp is added, ice bath removed and were reacted for 1 h as rxn soln warms to RT. Rxn quenched with water 10 min after addition of TMSCl.	-TLC
5	(1: 6: 2)	Rxn done under Ar. DiiA and n-BL were reacted for 30 min. LDA soln was added to dmp via cannula and were reacted for 1 hr. TMSCl was added in small portions every 10 min until gone. An aliquot was taken out after each addition and a TLC was run. Rxn quenched with water after 25 min.	¹ H nmr in CDCl ₃ on VI300 -Mass Spec (Done by CIF) -TLC
6	(1: 6: 2)	Same as in Attempt 5. Except half of the rxn soln was quenched after 5 h. The other half of the rxn soln was put in a hot water bath (42 °C) and quenched after 20.5 h.	¹ H nmr in CDCl ₃ on VI300 -Mass Spec (done by CIF) -TLC
7	(1: 6: 2)	Rxn stopped due to fluxional n-BL concentration.	N/A

Note: DiiA= diisopropyl amine, n-BL= n-butyl lithium, dmp= 2,9-dimethyl-1,10-phenanthroline, TMSCL= trimethylsilyl chloride, rxn= reaction, RT= room temperature, LDA= lithium diisopropyl amide, soln= solution.

Reaction II (Lit ref: 43 and 46)

Scheme II

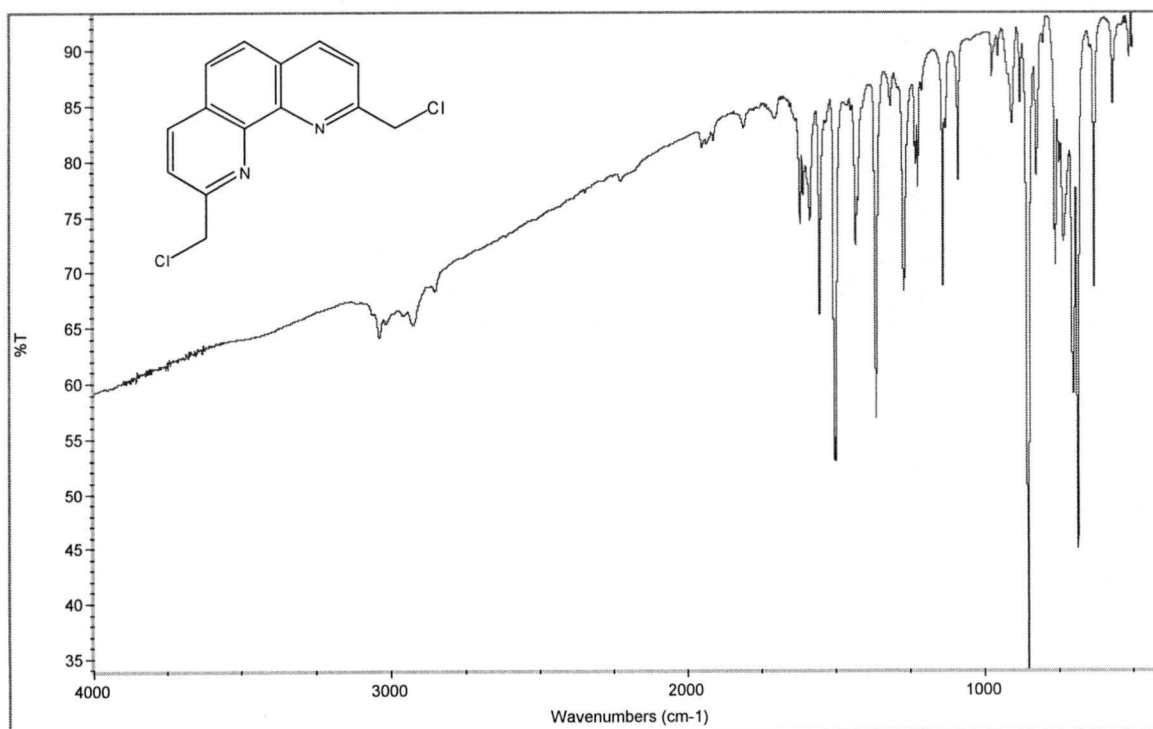
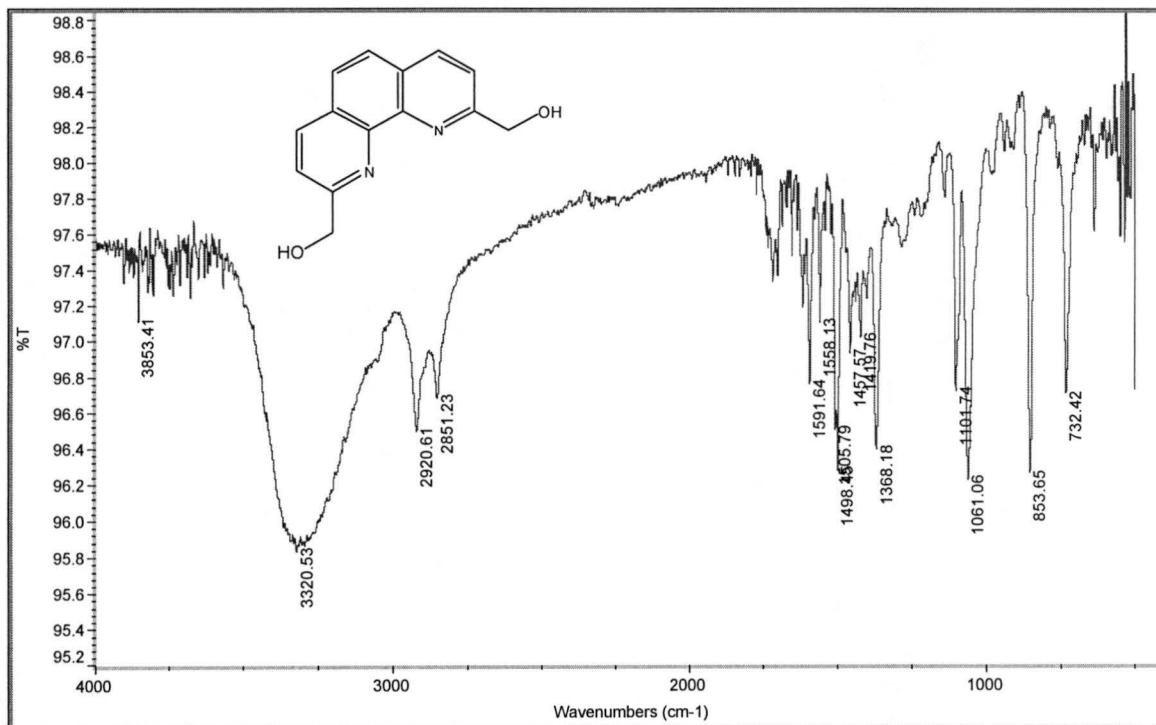


Conditions and Comments: Compounds 4-8 were prepared as described in ref 46 with the following exception. The 2,9-Bis(methoxycarbonyl)-1,10-phenanthroline was not purified by sublimation, but was extracted with CH_2Cl_2 , which was only partially successful. Also the 2,9-Bis(hydroxymethyl)-1,10-phenanthroline was not continuously extracted for 6 h, instead it was extracted 5x with CHCl_3 and the excess solids were then stirred in CHCl_3 for ~ 1-2 h, and filtered. Although the paper reports excellent yields for each part of this synthesis, the reported yields were much higher than experimentally achieved. The experimentally obtained yields are reported in Table II. The sequential nature of this synthesis combined with lower yields, and time commitment made this set of reactions an impractical method of preparation for the cmp and bmp ligands. When preparing bmp (9) the literature procedure from ref 43 was used. Since Br is a better leaving group than Cl, the synthetic goal of trials 2 and 3 was the synthesis of bmp. However, the last step in the synthesis (conversion of 7 to 9) often has a very low yield of product 9, presumably due to back reaction to 7 and side reactions. Often any product obtained in this step was too small to purify or lost during purification. ^1H NMR, and TLC were used to characterize all of synthesized compounds. Mass spec and IR were also used for characterization.

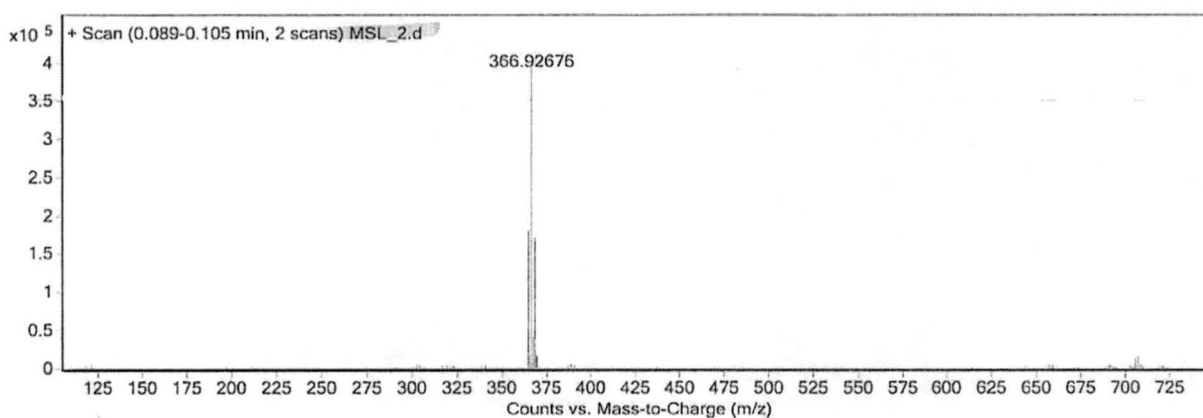
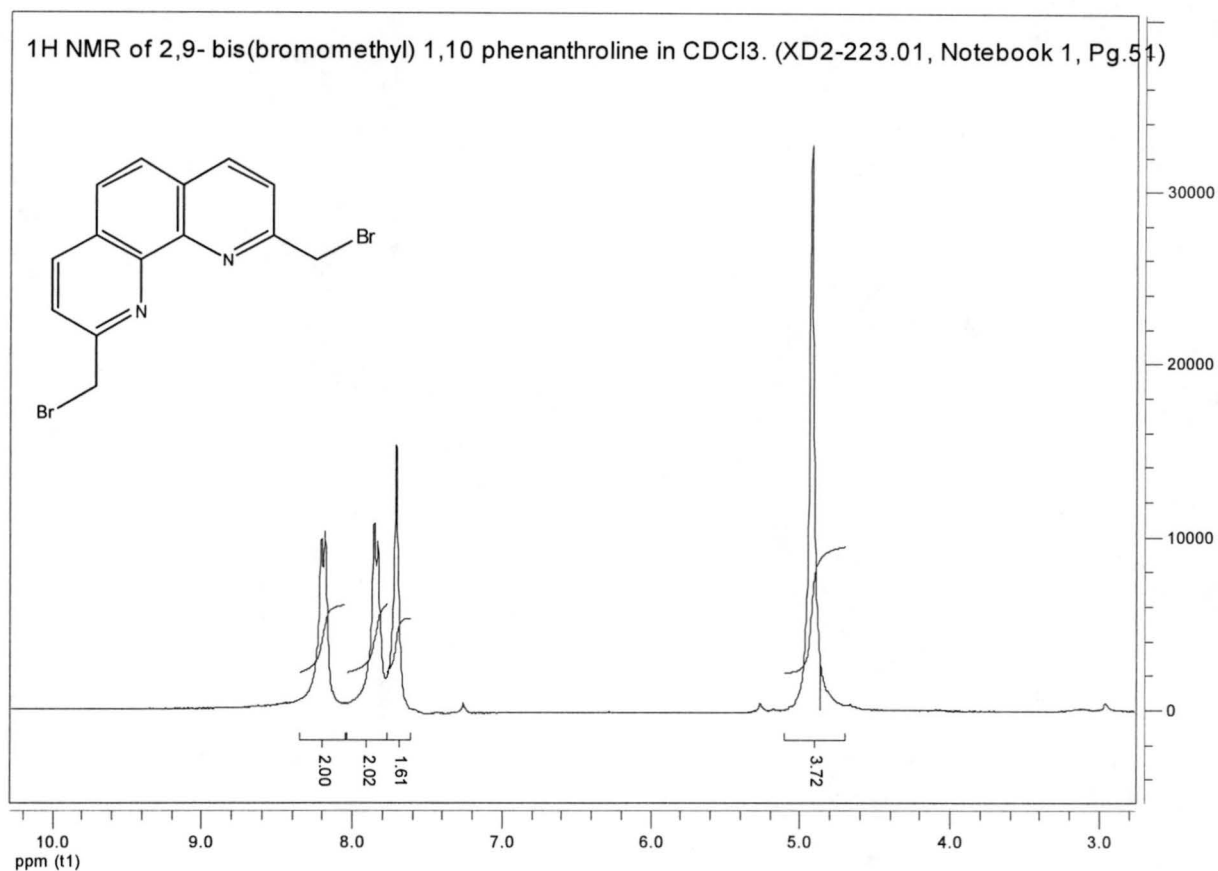
Table II. Experimentally obtained yields for several different trials of the synthesis of compounds 5-9.

Products	Literature Reported Yields (%)	Experimentally Obtained Yields (%)		
		Trial 1	Trial 2	Trial 3
5	100	53.35	68.96	67.57
6	95	79.87	42.11	82.82
7	95	59.55	32.87	49.55
8	72	53.99	-	-
9	79 (crude yield reported)	-	42.57	-
Overall % Yield of cmp or bmp	51.33	13.70	4.06	N/A

Characterization of Cmp Trial 1: The ^1H NMR of the 2,9-Bis(hydroxymethyl)-1,10-phenanthroline and 2,9-bis(chloromethyl)-1,10-phenanthroline are virtually identical. Therefore, IR spectroscopy was used to characterize the cmp complex by the disappearance of the strong, broad $-\text{OH}$ stretching frequency ($\sim 3000\text{-}4000\text{ m}^{-1}$). Admittedly, these spectra are not extremely compelling evidence.



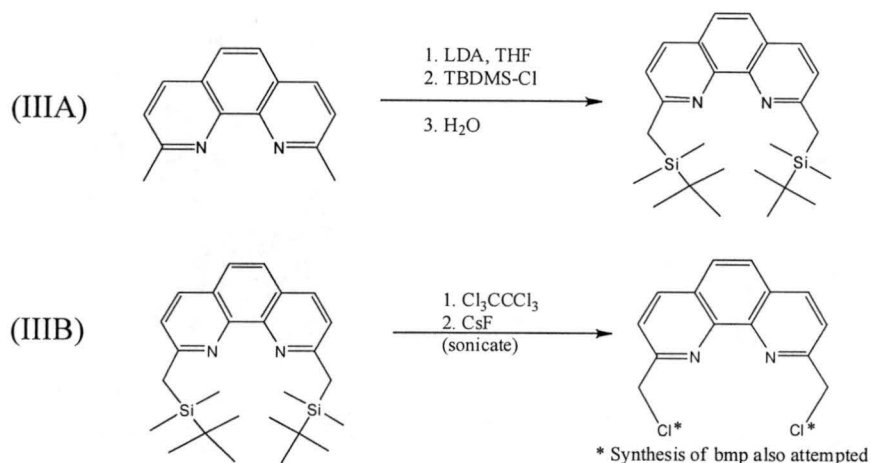
Characterization of bmp (Trials 2 and 3): The bmp was characterized by ^1H NMR in CDCl_3 (either VMI300 or VI300), mass spec, and TLC for Trial 1 and 2. Unfortunately, the product of Trial 2 was extremely impure, therefore spectra shown below are from the product of Trial 1.



Note: ChemBioDraw Ultra v.11.0.1 predicts that the exact mass of bmp is 363.92 amu, molecular weight is 366.05 amu and the m/z : 365.92 (100%), 363.92 (51.4%), 367.92 (48.7%), 366.92 (15.9%), 364.92 (8.2%), 368.92 (7.4%), 367.93 (1.1%). Also note that an artifact caused in printing (horizontal line) was removed using Lexmark Photo Editor.

Reaction III (Lit ref: 44,45,47)

Scheme III



Conditions and Comments: Reaction IIIA was done exactly as described in ref 45 with the following exceptions: The reaction was quenched with D₂O for Trial 1. This reaction was characterized by ¹H nmr (VI300), mass spec, and melting point (~77-78 °C). Rxn IIIB was done similarly to refs 44 and 47 with the following exceptions: Trial 1- hexachloroethane (Cl₃CCCl₃) was used instead of dibromotetrafluoroethane for making cmp. The reaction was done in acetonitrile, run for ~ 21.5 h, and not sonicated. The product was extracted with EtOAc (3x) and, after a column was run, extracted again with CH₂Cl₂/MeOH, rotovapped to ~2/3 of the original volume, then recrystallized from the extract solution in the refrigerator. Trial 2- Done as in refs 44 with the following exceptions: using Cl₃CCCl₃, and heated to 67 °C for ~ 5 h, then run overnight at ~43 °C. The product was purified by dissolving in hexanes, filtering, gathering solids, dissolving resulting solids in MeOH, filtering through celite, cooled in freezer to crash out medium polarity solids. Resulting solids were run through a silica using CH₂Cl₂:EtOAc eluent. The collected fractions were rotovapped to ~1/6 of the original volume, hexanes were added and put in freezer. Solids were collected and dried in vacuo. TLC was used to follow the purification process. Product was characterized by ¹H nmr in CDCl₃ (VI400) and mass spec. For the synthesis of bmp, the reaction was done exactly as in ref 44 except the reaction was run for 23 h and heated for the last 7 hours. Reaction followed by TLC. Resulting solids were also put through similar purification process as in Trial 2 of cmp synthesis. A column was run and gathered fractions were recrystallized from MeOH. No characterization has been done on this product at this time, but is planned.

Table III. Experimentally Observed Yields of Cmp

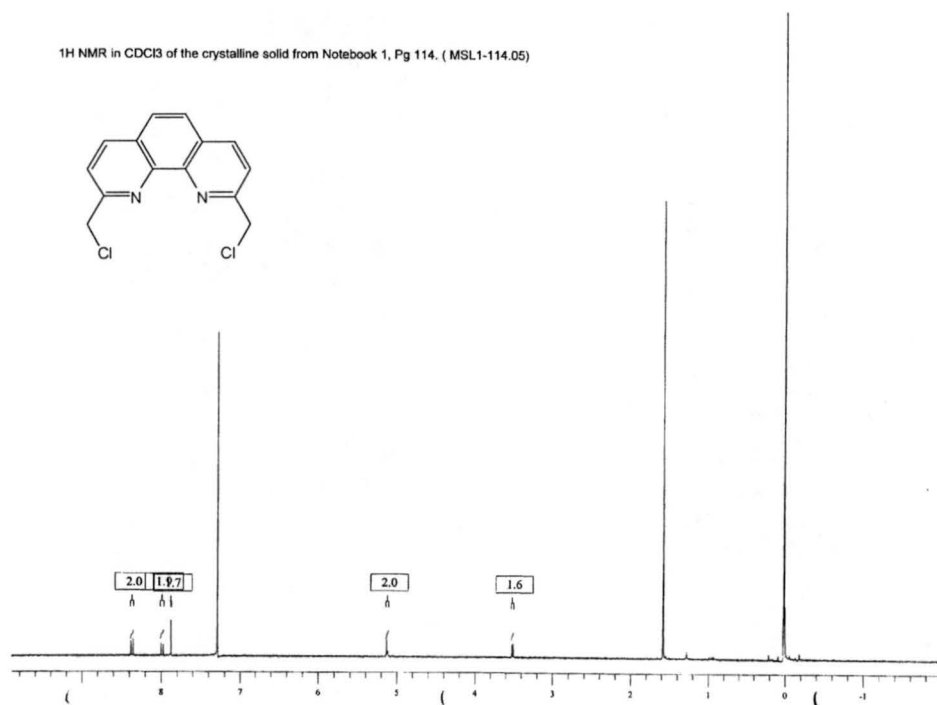
Yields	Experimental Trials				
	III A		IIIB (cmp)		IIIB (bmp)
	Trial 1	Trial 2	Trial 1	Trial 2	Trial 1
Literature Reported Yields (%)	98		ref 44= 71% (bmp); ref 47 = 91%(*)		71%
Experimentally Observed Yields (%)	<99	100 [‡]	Not calculated		30.77
Overall % Yield of cmp or bmp	-		-		≥30.77

* This yield was reported for the synthesis of 4,4'-Bis(chloromethyl)-2,2'-bipyridine.

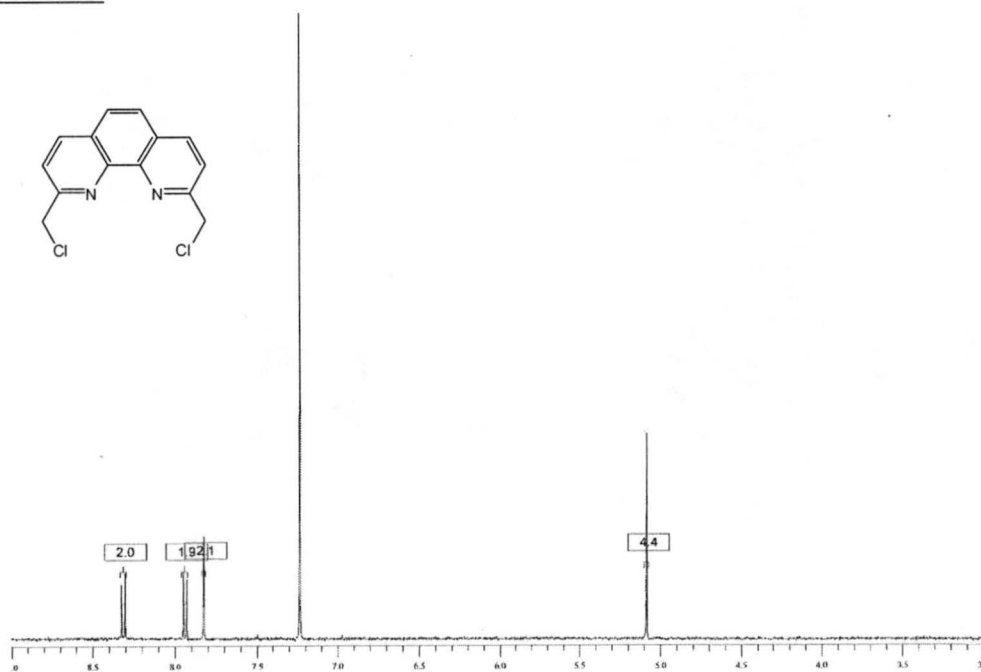
[‡] Increased yields possibly due to residual solvent.

Characterization of cmp: This reaction was characterized by ^1H NMR in CDCl_3 (VI300) and mass spec. Impurities at 0 ppm and ~ 1.5 ppm were in both spectra, but in Trial 2 the images was cropped.

IIIB(cmp): Trial 1



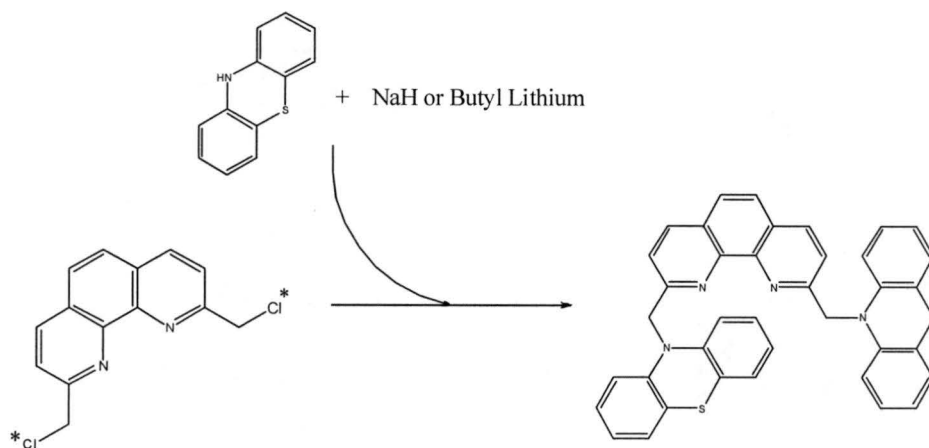
IIIB(cmp): Trial 2.



Section II: All Relevant Details for Attempted Syntheses of 2,9-Bis[(Phenothiazine)methyl]-1,10-Phenanthroline(bPZmp) and the Phenoxazine (bPOmp) Analog.

Reaction IV (Lit Ref: 7)

Scheme IV



* Also used 2,9 bis(bromomethyl) 1,10 phenanthroline

Conditions and Comments: This type of nucleophilic displacement reaction was suspected to be the most probable synthesis of the bPZmp and bPOmp ligands. Therefore several variations on this reaction were attempted. The general reaction conditions are as follows: This reaction was performed under an inert atmosphere (N₂ or Ar). Sodium hydride (NaH) or n-BL were added to a solution of PTZ or POZ in THF and reacted for 30 min at 0 °C (ice bath). The bmp (or cmp) ligand was dissolved in THF at room temperature and added to the PTZ solution via cannula. The reaction was reacted at different temperatures and times depending on the specific experiment. The reaction was quenched and product was purified by several different methods. The changes to the general reaction scheme described above for each individual trial will be outlined in the following section.

Table IV: Stoichiometric relationships and specific reagents used for each experiment. Order of addition indicates if the deprotonated PXZ (dPXZ) was added to the cmp (or bmp) or vice versa.

Trial	Stoichiometry (bmp(or cmp):NaH or n-BL: PXZ)	Order of addition
1	1 (cmp): 2 (n-BL (2.5 M)): 2 (PTZ)	Cmp → PTZ
2	1 (bmp): 15 (NaH (60%)) : 15 (PTZ)	Bmp → PTZ
3	1 (bmp): 15 (NaH (60%)) : 15 (PTZ)	Rxn contaminated and aborted
4	1 (bmp): 5 (n-BL (1.6 M)): 6 (PTZ)	Bmp → PTZ
5	1 (bmp): 3 (n-BL (1.6 M)): 3 (PTZ)	Bmp → PTZ
6	1 (bmp) : 1.2 (NaH (dry, 97%)): 3 (PTZ)	Bmp → PTZ
7	1 (deuterated-cmp= d-cmp): 2 (n-BL (1.38 M)*: 3 (PTZ)	Cmp → PTZ

* 1.6 M n-BL was titrated with menthol. The actual molarity was determined to be 1.38 M.

Table IVA: Changes to generalized reaction conditions for each experiment. The yields are not given because none of these experiments yielded the desired product. Only the changes to the reactions scheme are outlined, everything else is the same as described above. All ^1H NMR was performed on the VI300 or VMI300 unless otherwise indicated. All glassware, solvents and relevant materials were degassed. Glassware was stored in oven until use.

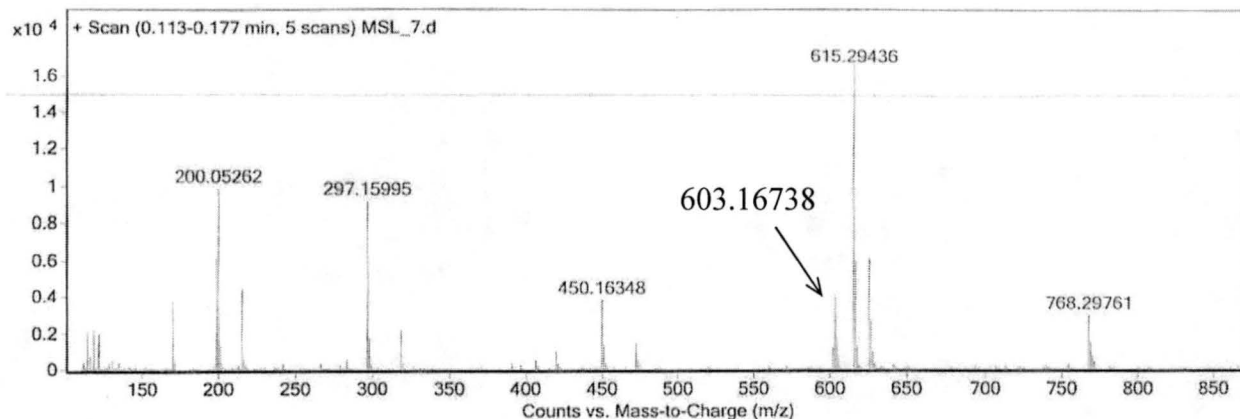
Trial	Reaction Conditions	Characterization
1	Run under N_2 . PTZ and n-BL were reacted for 1h. After cmp was added the rxn was kept on an ice bath and run overnight so the rxn warmed to RT. The rxn was quenched [†] . The product was extracted with CHCl_3 (x5) and run through a silica column (flushed with 1% triethylamine (TEA)/hexanes, then hexanes; eluent: hexanes/ CH_2Cl_2).	^1H nmr in alumina filtered CDCl_3 -TLC
2	Run under N_2 . PTZ and NaH were reacted for 2 h (bright yellow, clear soln). After bmp was added, the rxn was run overnight at RT. Rxn was quenched and product was separated by column chromatography (silica) [†] .	^1H nmr in alumina filtered CDCl_3 -TLC
3	The color of the PTZ/NaH soln indicated possible contamination so the rxn was aborted.	-N/A
4	Run under N_2 . PTZ and n-BL were reacted for 30 min (bright yellow, clear soln). TLC was used to follow the rxn after the bmp was added (rxn soln dark green). Rxn was quenched with MeOH right after the rxn soln turned dark brown. Product was extracted with diethyl ether (x3). A silica column was run (flushed with hexanes; eluent: ether:hexanes (1:50)).	^1H nmr in d-acetonitrile -TLC
5	Run under N_2 . PTZ and n-BL were reacted for 30 min (bright yellow, clear soln). After bmp was added, the ice bath was changed to a dry ice/acetone bath ($\sim -78^\circ\text{C}$, dark red/brown soln). Rxn was quenched with MeOH after 20 min. Rxn soln dried in vacuo, rinsed with hexanes, and rinsed with ether.	^1H NMR in d-DMSO -TLC
6	Run in dry box. PTZ and NaH reacted for 20 min (light yellow-red soln). After bmp was added the rxn was stirred at RT for 3 h. After 3 h the temperature was gradually increased until reflux. Rxn was refluxed overnight and then quenched w/ EtOH. Solids were collected and dried in vacuo to give orange crystals, which were rinsed with pentane. Crystals turned dark red/brown over time.	^1H NMR in alumina filtered CDCl_3 - Mass Spec (See IV: Trial 6) -TLC
7	Run under Ar. PTZ and n-BL were reacted for 30 min (bright green-yellow, clear soln) at -78°C . d-cmp was added (soln clear, light yellow/brown). 0.6 ml d^6 -bz was added to rxn mix. An aliquot was put into an air-sensitive NMR tube, and kept at the same conditions as the rxn soln. Rxn was run at -78°C for 5 h, then taken off of the dry ice/acetone bath and run overnight warming to RT (soln more brown). After 22 hrs the rxn was heated to 45°C , run for 8.5 h (soln more brown, ppt formed) and then quenched with glacial acetic acid. Rxn was followed by ^1H nmr.	^1H nmr in d^6 -benzene (d^6 -bz) -Mass Spec (See IV: Trial 7)

[†] Work performed in collaboration with Di Xue and many details were not disclosed

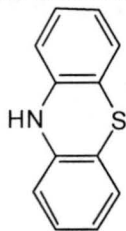
Important Spectra from Trials 6 and 7 in Table IV A. The following spectra help elucidate the reason why the bPZmp is not being formed by the previous reactions.

IV: Trial 6

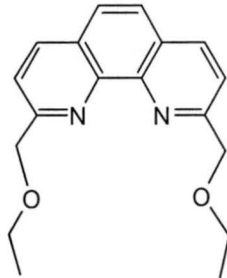
Comments: The peak at m/z : 603.16738 is known, due to more focused scan from m/z : 580-655.



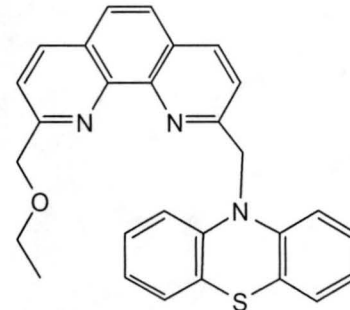
m/z : 200.05



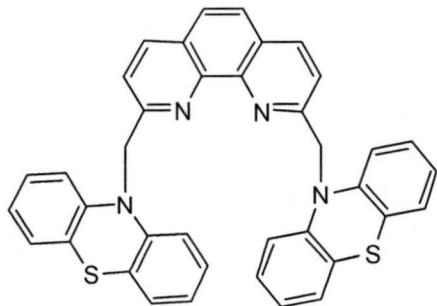
m/z : 297.16



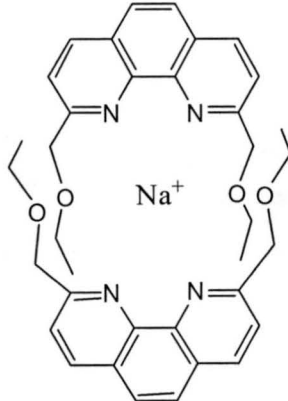
m/z : 450.16



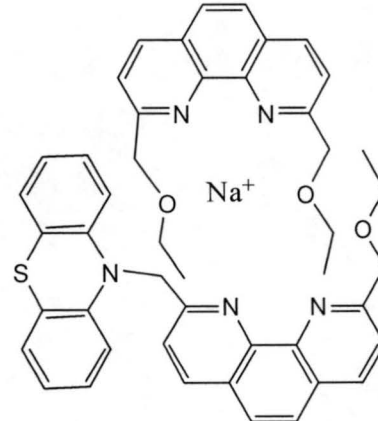
m/z : 603.17



m/z : 615.29

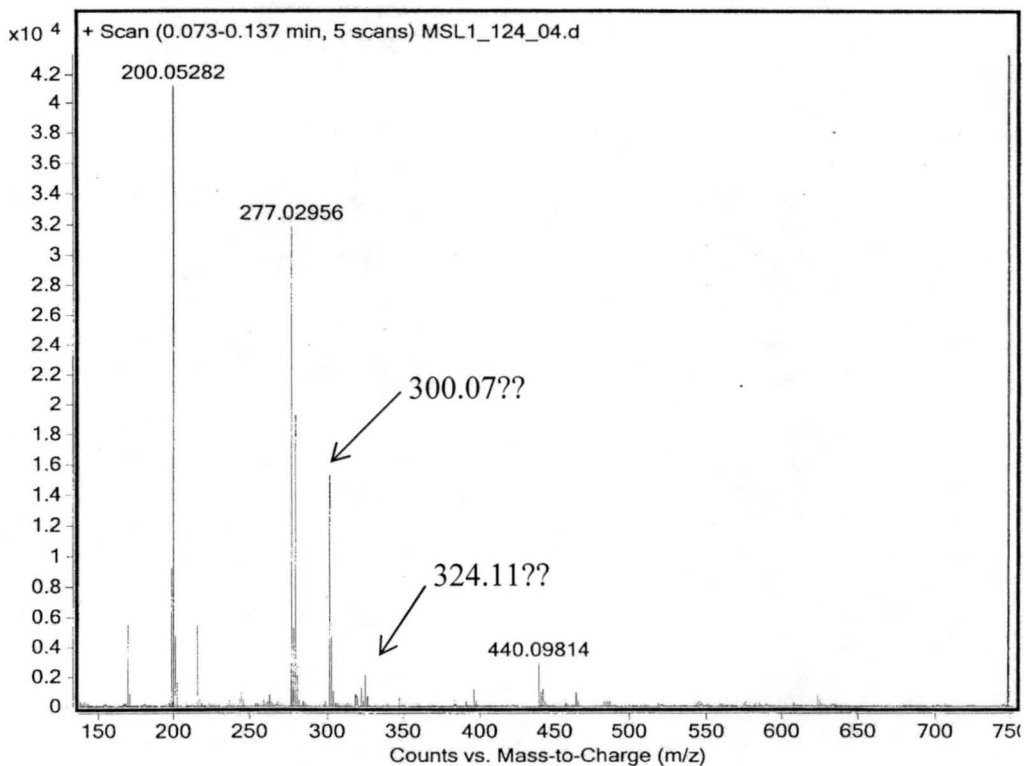


m/z : 768.30

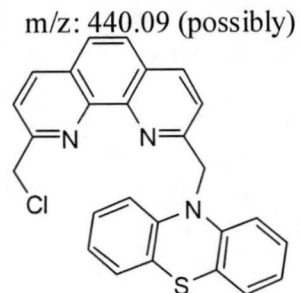
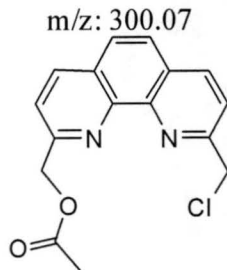
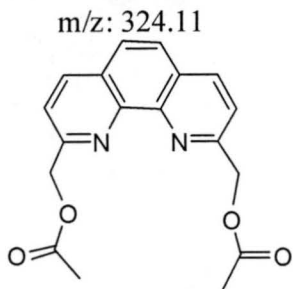
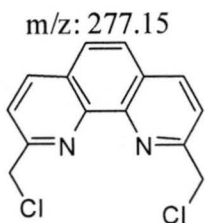


IV: Trial 7

Comments: It is not certain that the peaks at m/z : 300.07 and 324.11 actually correspond to the structures below since this was a nominal mass scan and the peaks were not labeled.

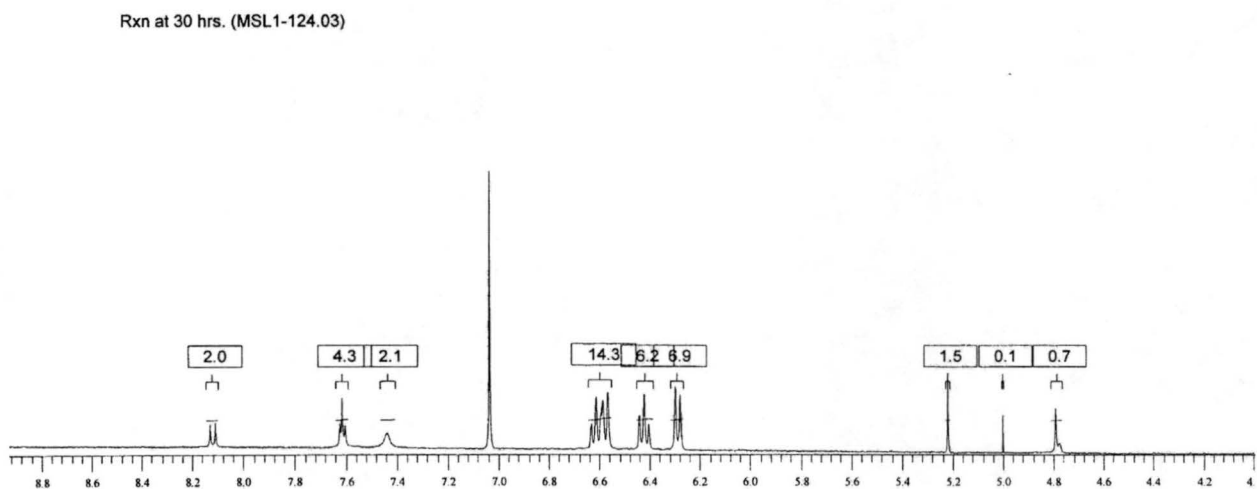
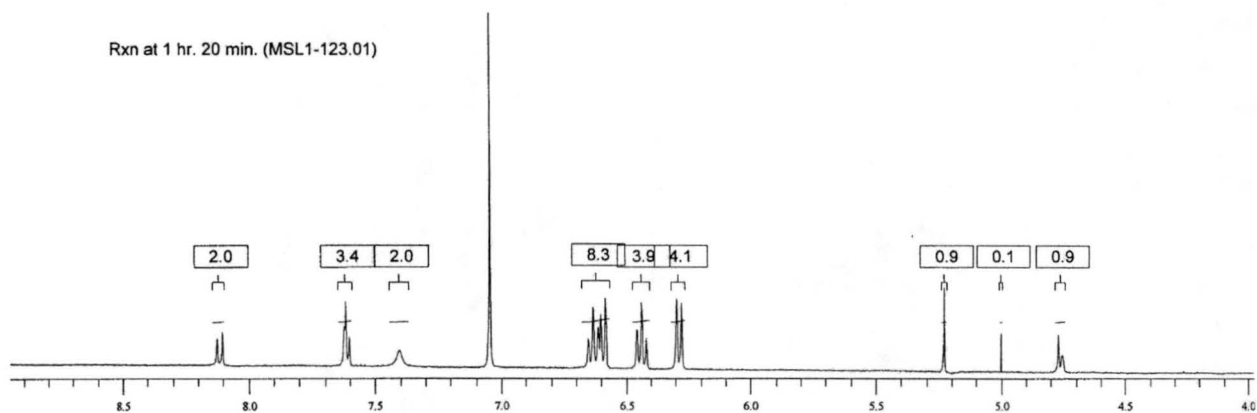


m/z : 200.05 = PTZ



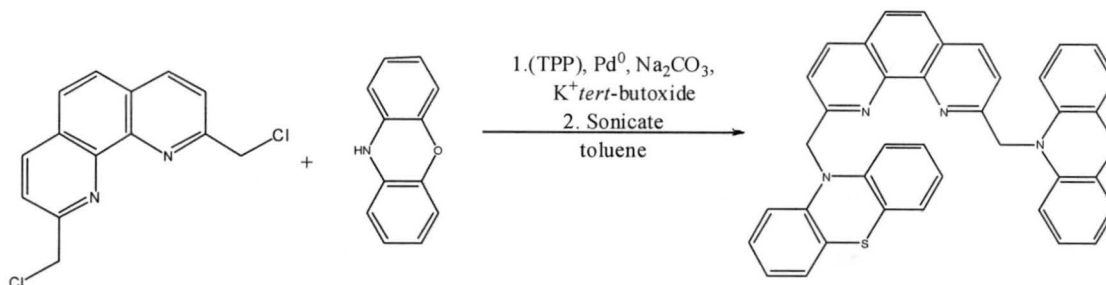
IV: Trial 7

As can be seen by the first and last ^1H NMR (VI400) spectra, no appreciable reaction occurred over the span of 30 h.



Reaction V (Lit ref 49)

Scheme V



Conditions and Comments: Stoichiometry; [1(cmp): 6.5 (Na₂CO₃): 3(POZ): 10(TPP)]. This reaction was run under Ar. Cmp and POZ were dissolved in dry toluene. The tetrakis(triphenylphosphine)Pd⁰, Na₂CO₃ and triphenylphosphine (TPP) were added to the reaction mixture, which was sonicated and heated to ~80 °C. After ~30 min the solution turned a reddish hue. After ~2h, TLC indicated that the reaction was not proceeding quickly so one microspatula tip full of potassium tert-butoxide (K-tB) was added and the reaction mixture turned reddish brown. The reaction was run for 3.5 h at ~80 °C, the heat and sonication was turned off and the reaction mixture was stirred overnight. The heat (~57 °C) and sonication were turned back on after a total reaction time of 17 h. The reaction was allowed to run for ~2.5 h longer. Another microspatula tip full of K-tB was added and the solution turned dark, bright cherry red. The reaction was quenched with glacial acetic acid after a total reaction time of ~20 h. Hexanes was added to the solution in order to rinse off non-polar impurities. The solids were gathered dissolved in CH₂Cl₂, more hexanes was added and the solution was put in the freezer. The resulting ppt was gathered, dissolved in CH₂Cl₂, MeOH was added, and the CH₂Cl₂ was rotovapped off to force dissolution into MeOH. The solution was then put into freezer. A red solid ppt formed and was collected for characterization. Although this was the crude product an ¹H NMR (VI400) and mass spec were taken (See V: Trial 1). This sample was combined with the product yielded from reaction VI and a column was run as described in the Experimental section.

Reaction VI (Lit ref 49)

Scheme VI

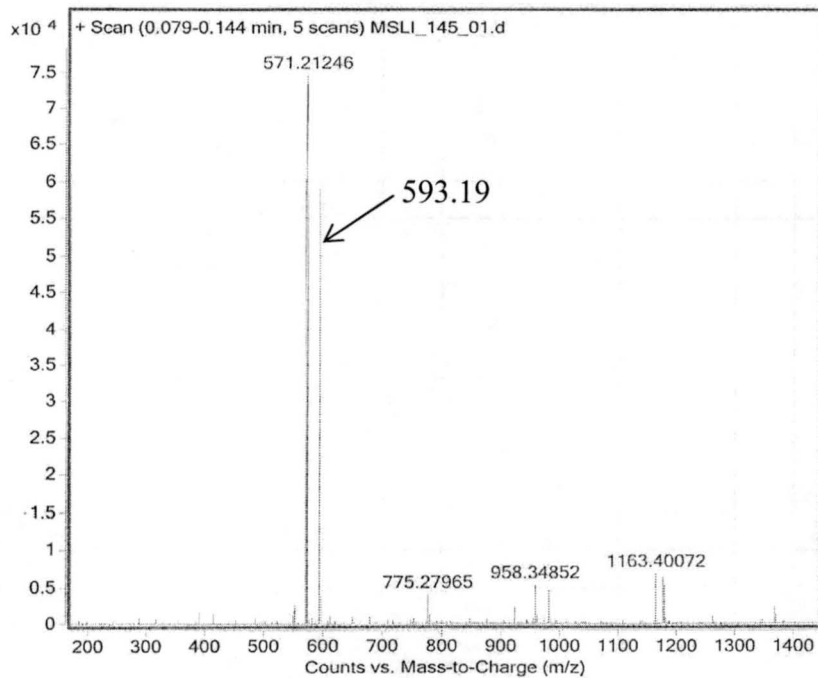
Same as shown above.

Conditions and Comments: Stoichiometry; [1(cmp): 3 (POZ)]. The main change from Reaction V to Reaction VI is that no tetrakis(triphenylphosphine)Pd⁰, Na₂CO₃ and triphenylphosphine were used. The details of this reaction are outlined in the Experimental section.

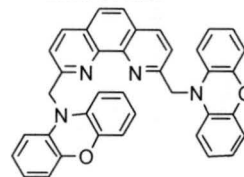
Important Spectra from Reactions V and VI

V: Trial 1

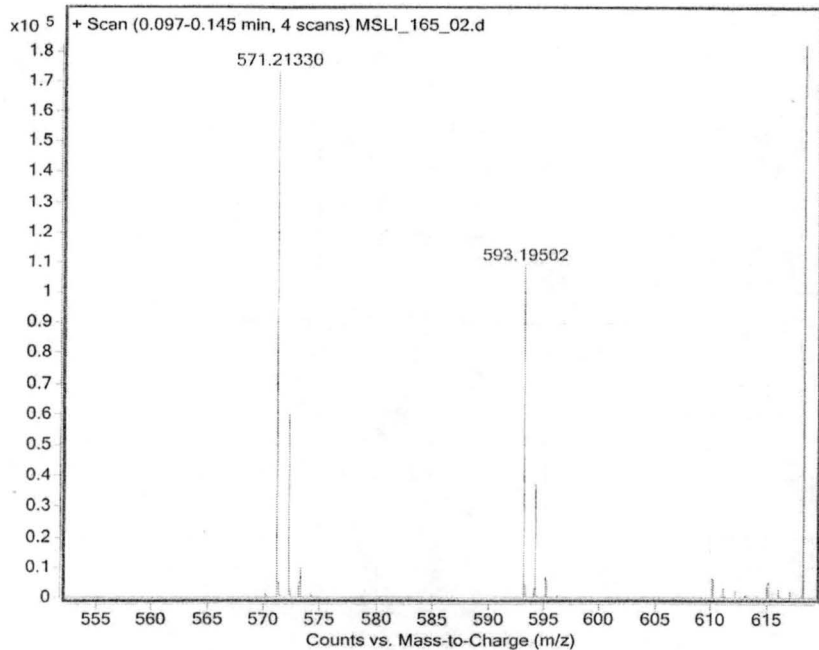
Comments: The peak at m/z : 593.19 is known due to a more focused scan from m/z : 530-660.



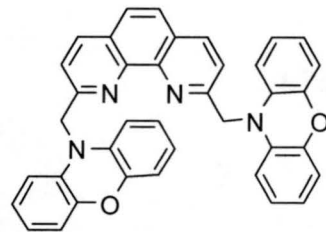
m/z : 571.21



VI: Trial 1



m/z: 571.21



m/z: 593.19

